RESEARCH

UDOT Keeping Utah Moving

Utah Department of Transportation - Research Division
4501 South 2700 West - P.O. Box 148410 - SLC,UT 84114-8410

Report No. UT-15.05

DATA-DRIVEN FREEWAY PERFORMANCE EVALUATION FRAMEWORK FOR PROJECT PRIORITIZATION AND DECISION MAKING

Prepared For:

Utah Department of Transportation
Research Division

Submitted By:

University of Utah
Department of Civil and Environmental Engineering

Authored By:

Xiaoyue Cathy Liu
Zhuo Chen

DISCLAIMER

The authors alone are responsible for the preparation and accuracy of the information, data, analysis, discussions, recommendations, and conclusions presented herein. The contents do not necessarily reflect the views, opinions, endorsements, or policies of the Utah Department of Transportation or the U.S. Department of Transportation. The Utah Department of Transportation makes no representation or warranty of any kind, and assumes no liability therefore.

ACKNOWLEDGMENTS

The authors acknowledge the Utah Department of Transportation (UDOT) for funding this research, and the following individuals from UDOT on the Technical Advisory Committee for helping to guide the research:

- Eric Rasband
- John Haigwood
- Tam Southwick
- Kelly Burns
- Glenn Blackwelder
- Jeff Williams
- Cody Oppermann

TECHNICAL REPORT ABSTRACT

1. Report No. UT- 15.05	2. Government Accession No. N/A	3. Recipient's Catalog No. N/A
4. Title and Subtitle DATA-DRIVEN FREEWAY PERFORMANCE EVALUATION FRAMEWORK FOR PROJECT PRIORITIZATION AND DECISION MAKING		5. Report Date March 31, 2015 6. Performing Organization Code
7. Author(s) Xiaoyue Cathy Liu and Zhuo Chen		8. Performing Organization Report No.
9. Performing Organization Name and Address University of Utah Department of Civil and Environmental Engineering 110 Central Campus Drive, Salt Lake City, UT 84112		10. Work Unit No. 8RD1523H 11. Contract or Grant No. 14-8691
12. Sponsoring Agency Name and Address Utah Department of Transportation 4501 South 2700 West P.O. Box 148410 Salt Lake City, UT 84114-8410		13. Type of Report & Period Covered Draft Final Report Jan 2014 to Feb 2015 14. Sponsoring Agency Code PIC No. AM14.02

15. Supplementary Notes

Prepared in cooperation with the Utah Department of Transportation and the U.S. Department of Transportation, Federal Highway Administration

16. Abstract

This report describes methods that potentially can be incorporated into the performance monitoring and planning processes for freeway performance evaluation and decision making. Reliability analysis is conducted on the selected I-15 corridor by employing congestion frequency as the performance measure and hot spots during peak hours are identified through sensitivity analysis. A data-driven algorithm combining spatiotemporal analysis and shockwave theory is developed and applied to historical traffic data and incident records to determine the secondary incidents. The results show that the occurrence of secondary incidents is highly related to weather and roadway conditions. Incident-induced delay is further quantified through spatiotemporal pattern recognition. The average delay induced by incidents aligns well with the incidents' severity and impact. There were several hot spots suffering from higher delays and are explored in further details. A statistical mechanism is developed to determine the adverse weather impact on travel. Using the weather records in 2013 and mapping with the PeMS traffic database, the volume and delay under normal condition are estimated and compared with the condition under adverse weather. The analysis of different roadway conditions reveals that the general parabolic pattern of speed and volume disappear under severe adverse weather condition. The mechanism is able to identify the causes for reduced volume under a variety of scenarios through empirical data, either due to roadway capacity reduction or travel demand reduction.

17. Key Words Reliability, incident-induced delay, secondary incident, weather impact analysis, data-driven approach		18. Distribution Statement Not restricted. Available through: UDOT Research Division 4501 South 2700 West P.O. Box 148410 Salt Lake City, UT 84114-8410 www.udot.utah.gov/go/research		23. Registrant's Seal N/A
19. Security Classification (of this report) Unclassified	20. Security Classification (of this page) Unclassified	21. No. of Pages 59	22. Price N/A	

TABLE OF CONTENTS

LIST OF TABLES v
LIST OF FIGURES vi
UNIT CONVERSION FACTORS vii
LIST OF ACRONYMS viii
EXECUTIVE SUMMARY 1
1.0 INTRODUCTION 3
1.1 Problem Statement 3
1.2 Objectives 5
1.3 Scope 6
1.4 Outline of Report 7
2.0 LITERATURE REVIEWS 8
2.1 Overview 8
2.2 Performance Metrics for Reliability Analysis 8
2.3 Secondary Incident Identification and Incident-Induced Delay 10
2.4 Evaluation of Adverse Weather Impact 12
2.5 Summary 12
3.0 RESEARCH METHODS 13
3.1 Overview 13
3.2 Performance Metrics for Reliability Analysis 13
3.3 IID 16
3.3.1 Secondary incident Identification 17
3.3.2 Spatial and temporal analysis for incident's impact extent 20
3.3.3 Pattern matching to determine the recurrent congestion delay 24
3.4 Evaluation of Adverse Weather's Impact 26
3.5 Summary 27
4.0 DATA COLLECTION 28
5.0 DATA ANALYSIS 29
5.1 Overview 29
5.2 Performance Metrics for Reliability Analysis 29

5.3 Secondary Incident Identification 31
5.4 IID 33
5.5 Adverse Weather's Impact 36
5.6 Summary 41
6.0 CONCLUSIONS 43
6.1 Summary 43
6.2 Findings 44
6.2.1 Congestion Frequency Index 44
6.2.2 Secondary Incident Occurrence 44
6.2.3 Hotspots on I-15 Corridor 44
6.2.4 Mechanism of Adverse Weather Impacting Traffic 45
6.3 Recommendations 45
REFERENCES 46

LIST OF TABLES

Table 2-1 Travel Time Reliability Measures from Previous Works.....9
Table 5-1 Operator's Estimation of Incident Information.....33
Table 5-2 Comparison of Estimated Delay and Operator's Estimated Delay.....34
Table 5-3 Signs of $\boldsymbol{\Delta F}$ and $\boldsymbol{\Delta D}$ for Combinations of C1, C2, C3, C4.....39

LIST OF FIGURES

Figure 3-1 I-15 Study Corridor 13
Figure 3-2 Speed Profile at 15th, 50th, and 85th Percentiles across Study Corridor 14
Figure 3-3 Speed-Flow Relationship using Empirical Data Collected 15
Figure 3-4 Congestion Frequency Heat Map under Different Speed Thresholds 16
Figure 3-5 Flowchart of Incident-Induced Delay Estimation 17
Figure 3-6 Example of Incident's Impact at MP 305 on July, 15, 2013 18
Figure 3-7 Example of Primary and Secondary Incident Matching 20
Figure 3-8 Speed-Flow Plot with Van Aerde's Curve Fitting 21
Figure 3-9 Sample Delay Histogram for Incident-Free Scenario 23
Figure 3-10 Examples of VHT Pattern Matching 25
Figure 5-1 Congestion Frequency and Speed Profile at 15th, 50th, and 85th Percentiles across I-15 Study Corridor 31
Figure 5-2 Histogram of Secondary Incident Induced 32
Figure 5-3 Secondary Incident Distribution by Month 32
Figure 5-4 Relationship between Estimated Delay with Impact/Severity 34
Figure 5-5 Summary of Total Delay, IID, and Number of Incidents along the Study Corridor 35
Figure 5-6 Locations of Incident Hotspots 36
Figure 5-7 Histogram of Weather Observations by Road Condition 37
Figure 5-8 Histogram of Weather Observations by Sky Condition 37
Figure 5-9 Traffic Flow Vs Speed Plots under Different Road Conditions 38
Figure 5-10 Scatter Plots of $\boldsymbol{\Delta F}$ Vs. $\boldsymbol{\Delta D}$ During Peak and Non-Peak Hours 40
Figure 5-11 Comparison of Pie Plots during Peak and Non-Peak Hours 40
Figure 5-12 Combination Frequency during Peak Hours under Different Road Conditions. 41

UNIT CONVERSION FACTORS

SI* (MODERN METRIC) CONVERSION FACTORS

APPROXIMATE CONVERSIONS TO SI UNITS

Symbol	When You Know	Multiply By	To Find	Symbol
		LENGTH		
in	inches	25.4	millimeters	mm
ft	feet	0.305	meters	m
yd	yards	0.914	meters	m
mi	miles	1.61	kilometers	km
		AREA		
in^2	square inches	645.2	square millimeters	mm^2
ft^2	square feet	0.093	square meters	m^2
yd^2	square yard	0.836	square meters	m^2
ac	acres	0.405	hectares	ha
mi^2	square miles	2.59	square kilometers	km^2
		VOLUME		
fl oz	fluid ounces	29.57	milliliters	mL
gal	gallons	3.785	liters	L
ft^3	cubic feet	0.028	cubic meters	m^3
yd^3	cubic yards	0.765	cubic meters	m^3
		NOTE: volumes greater than 1000 L shall be shown in m^3		
		MASS		
oz	ounces	28.35	grams	g
lb	pounds	0.454	kilograms	kg
T	short tons (2000 lb)	0.907	megagrams (or "metric ton")	Mg (or "t")
		TEMPERATURE (exact degrees)		
°F	Fahrenheit	5 (F-32)/9 or (F-32)/1.8	Celsius	°C
		ILLUMINATION		
fc	foot-candles	10.76	lux	lx
fl	foot-Lamberts	3.426	$candela/m^2$	cd/m^2
		FORCE and PRESSURE or STRESS		
lbf	poundforce	4.45	newtons	N
lbf/in^2	poundforce per square inch	6.89	kilopascals	kPa

APPROXIMATE CONVERSIONS FROM SI UNITS

Symbol	When You Know	Multiply By	To Find	Symbol
		LENGTH		
mm	millimeters	0.039	inches	in
m	meters	3.28	feet	ft
m	meters	1.09	yards	yd
km	kilometers	0.621	miles	mi
		AREA		
mm^2	square millimeters	0.0016	square inches	in^2
m^2	square meters	10.764	square feet	ft^2
m^2	square meters	1.195	square yards	yd^2
ha	hectares	2.47	acres	ac
km^2	square kilometers	0.386	square miles	mi^2
		VOLUME		
mL	milliliters	0.034	fluid ounces	fl oz
L	liters	0.264	gallons	gal
m^3	cubic meters	35.314	cubic feet	ft^3
m^3	cubic meters	1.307	cubic yards	yd^3
		MASS		
g	grams	0.035	ounces	oz
kg	kilograms	2.202	pounds	lb
Mg (or "t")	megagrams (or "metric ton")	1.103	short tons (2000 lb)	T
		TEMPERATURE (exact degrees)		
°C	Celsius	1.8C+32	Fahrenheit	°F
		ILLUMINATION		
lx	lux	0.0929	foot-candles	fc
cd/m^2	$candela/m^2$	0.2919	foot-Lamberts	fl
		FORCE and PRESSURE or STRESS		
N	newtons	0.225	poundforce	lbf
kPa	kilopascals	0.145	poundforce per square inch	lbf/in^2

*SI is the symbol for the International System of Units. (Adapted from FHWA report template, Revised March 2003)

LIST OF ACRONYMS

BI	Buffer Index
DQT	Deterministic Queuing Theory
FHWA	Federal Highway Administration
HCM	Highway Capacity Manual
IID	Incident-Induced Delay
ITS	Intelligent Transportation System
MAP-21	Moving Ahead for Progress in the 21st Century Act
PeMS	Performance Measurement System
PI	Planning Time Index
SHRP 2	Strategic Highway Research Program
TATS	Traveler Advisory Telephone System
TIM	Traffic Incident Management
TOC	Traffic Operations Center
TTI	Travel Time Index
UDOT	Utah Department of Transportation

EXECUTIVE SUMMARY

This study aims at developing a set of performance metrics and computational methodologies that can be incorporated into operational management and planning process for investment decision making. This report details the work performed in this research project. The objectives of this project are to (a) quantify the impact of nonrecurring congestions, including incidents and weather; and (b) provide linkage between performance measures and decision making by using interpretative indicators to inform decisions.

Freeway performance measures are oftentimes considered in three dimensions: temporal aspect, spatial details, and source of congestion. This study looks at these dimensions from a holistic view and strives to describe the roadway conditions in support of investment decisions. We start by looking at the freeway network as a whole, and determining its overall condition. For example, where are the unreliable locations along a freeway corridor and how to measure the reliability/unreliability? To answer these questions, we developed a measure named congestion frequency, that is intuitive to use and consistent with the speed reliability measurement currently used by UDOT. Congestion frequency is defined as the percentage of time that speed drops below a certain threshold. By extracting traffic information from historical archived data in PeMS, this indicator can be calculated and sensitivity analysis is conducted to choose the proper threshold.

A methodological framework is developed to quantify the incident-induced delay and identify the secondary incidents based on the empirical data collected. The framework acknowledges that each individual incident has different impact on the roadway both spatially and temporally due to varying traffic conditions, roadway geometries, and crash characteristics. Thus a data-driven algorithm is developed to determine the impact region for each incident. By heuristically searching the historical database and perform pattern matching to find the historical traffic condition that matches the incident scenario, the incident-induced delay is calculated and secondary incidents are identified. There were 109 primary incidents and 240 secondary incidents identified on the selected I-15 Northbound corridor during 2013. From the distribution of secondary incidents, it is observed that the occurrence of secondary incidents is highly related to weather condition. The incident-induced delay is influenced by severity, location, and time-of-day. A statistical mechanism is developed to determine the adverse weather impact on travel.

Utilizing the weather/roadway information provided by Traveler Advisory Telephone System (TATS) and PeMS, an algorithm is developed to map the traffic data with the weather database. It is concluded that during adverse weather, especially when the road is snow-covered, lower flow is associated with high delay during the peak period, indicating a reduction in speed. And the non-peak period has a significant reduction in delay comparing with the historical travel pattern which implies a reduction in demand.

1.0 INTRODUCTION

1.1 Problem Statement

With the burgeoning development of Intelligent Transportation System (ITS) over the past decades, it inspires the smart and efficient management of current roadway networks. One concern of freeway performance management is congestion, which can be attributable to recurring and nonrecurring causes. According to the 2012 Urban Mobility Report, urban congestion costs about $12.1 billion dollars and a total of 5.52 billion-hour delay in 2011 (Schrank, *et al*., 2012). Congestion has surely been growing over the past years. Transportation agencies are therefore actively seeking for ways to better monitor the traffic, identify bottlenecks, and respond efficiently and effectively to incidents. From an operations perspective, using a set of meaningful performance measures to obtain comprehensive assessment of the roadway system is one of the most effective solutions for congestion management. It is also critical to decision making. The Moving Ahead for Progress in the 21st Century Act (MAP-21) establishes a performance-based transportation program to guide the transportation capital investment and development. It thus enables the need to carry out a performance-based approach in evaluating the transportation system. Freeway networks play a very critical role in providing accessibility to a multitude of resources and serves as the backbone of a region's economic vitality. It is also the primary focus of operations agencies. Meanwhile, social and economic needs continue to shape the freeway network in turn with the rapid advancement of technology. It is therefore imperative to develop a data-driven freeway performance assessment framework that is able to link the performance measures with investment decisions.

Freeway performance measures are oftentimes considered in three dimensions: temporal aspects, spatial details, and source of congestion. Attention will be paid differently depending on the emphasis of specific agencies. For example, a senior leader would look at the performance from a holistic view to obtain the overall freeway network conditions. Traffic engineers may need to provide instantaneous operation decisions based on the source of congestion and time of day situation. Transportation planners might consider developing plans for alleviating congestion bottlenecks that are most critical to the entire network. In order to provide comprehensive and useful information to transportation agencies, the performance measures should be developed

incorporating the three dimensions mentioned above, as well as to effectively describe the roadway condition to support investment decisions. There is also a growing recognition in the transportation profession in recent years that performance measures should be viewed from both facility perspective for monitoring and management purposes and user perspective for customer experiences. To address this issue, performance measures need to be focused on both congestion (facility perspective) and mobility (user perspective) of the freeways.

There are seven potential sources that contribute to the travel unreliability identified by the FHWA SHRP 2 program. They are traffic incidents, weather, work zones, demand fluctuations, special events, traffic control devices, and inadequate base capacity. As one of the most critical contributors for traffic congestion, incidents account for approximately 50-60 percent delay on the U.S. highways (Bertini and McGill, 2003). In order to mitigate the impacts of incidents, it would be crucial for the incident management program to develop strategies that can effectively estimate the incident impact range and respond appropriately. The Traffic Incident Management (TIM) is a planned and coordinated process to detect, respond to, and remove traffic incidents and restore capacity as safely and quickly as possible. Accurate estimation of Incident-Induced Delay (IID) would assist with a better understanding of incident related congestion, thus to provide insights for effective TIM. Transportation agencies use information regarding IID for transportation planning purposes at different levels. Lately, the successful incorporation of reliability analysis into the planning and programming processes also demonstrates the importance of incident effects modeling (Cambridge Systematics, 2013). The estimation and prediction of IID can further be applied to traffic simulation calibration and validation. Accurate estimation of such delay can help identify appropriate decisions regarding incident response so that limited monetary and labor resources can be efficiently allocated. The IID is also essential for the development of active traffic management and integrated corridor management strategies. One critical step for the IID estimation is to determine the impact range of incidents in both spatial and temporal domains, which also makes it feasible to identify secondary incidents due to the congestion caused by a previous incident. According to FHWA, secondary incidents account for 20% of all incidents. And they include not only crashes, but also engine stalls, overheating and running out of fuel scenarios where vehicles experience unexpected delay due to the primary incidents. Secondary incident is another criterion for evaluating the effectiveness of TIM. According to Karlaftis *et al.* (1999), the likelihood of a

secondary crash increases by 2.8% for every minute that the primary incident continues to be a hazard.

Another major source for non-recurring congestion is adverse weather, which leads to changes in driver behavior to affect traffic flow. Adverse weather conditions have a major impact on the roadway safety and operations, which directly impact vehicle performance, pavement friction and roadway infrastructure. Due to reduced visibility and road friction, speeds are lowered and headways are increased when wet, snowy, or icy roadway surface conditions are present. To mitigate the impacts of adverse weather (e.g. rain, snow, ice, and fog), roadway weather management strategies are implemented by transportation agencies. For example, advisory strategies can provide information on predicted conditions. Control strategies can help restrict or regulate traffic flow through altering the traffic control devices in operation. Treatment strategies can minimize weather impacts by applying sand, salt, and anti-icing chemicals to pavement to increase traction. Studies that are able to explore the interaction between adverse weather and travel demand would benefit the weather management program to understand people's travel behavior and evaluate the effectiveness of these strategies.

1.2 Objectives

The primary objective of this research project is to quantify the impact of nonrecurring congestions. The nonrecurring sources in this study are focused on incidents and weather. IID is quantified through a data-driven algorithm. Previous research provided a general approach for the IID estimation, however, important features associated with incidents tend to be ignored in the estimation process, e.g. location-specific characteristics, congestion propagation and dissipation process in both spatial and temporal domains. Secondary incident identification is conducted by analyzing the congestion caused by a cluster of incidents via a binary contour method. The study also develops a mechanism to evaluate how adverse weather impacts the freeway network.

A secondary objective of this research project is to provide a linkage between performance measures and decision making by using interpretative indicators to inform decisions. The performance measures should be easily understood and have practical applications. The measures should tie to typical congestion levels, reliability and freeway

throughput to describe congestion/mobility performance of freeways, yet can be easily comprehended and related to by the general public based on their everyday experience.

1.3 Scope

The following major tasks are performed for this research, breaking down into three major components: *performance metrics development*, *IID analysis and secondary incident identification*, and *weather impact evaluation*:

- Develop a performance measure that can be used to describe the day-to-day variation of traffic conditions and is easily understandable by both practitioners and the general public.
- Develop a data-driven algorithm for secondary incident identification;
- Design an empirical methodological framework to quantify the IID on freeways, providing reference for incident management;
- Use pattern recognition to estimate non-recurrent congestion and demand reduction caused by adverse weather.

To conduct all the above mentioned tasks, it requires the support of a massive amount of historical and real time data from multiple sources and jurisdictions. The Performance Measurement System (PeMS) is a freeway performance measurement system used by Utah Department of Transportation (UDOT) and other transportation agencies, which is based on a subscription to the Iteris PeMS database. It contains a rich pool of information about traffic data and provides an excellent platform to both transportation practitioners and researchers. The system integrates various traffic data sources including traffic detectors, incident logs, vehicle classification data, and roadway inventory, etc. These traffic data have been automatically collected and archived and real-time information is updated from over 28,000 detectors. Meanwhile, UDOT maintains separate databases for vehicle incident tracking, weather conditions, and pavement conditions in the Traffic Operations Center (TOC). These datasets offer valuable information for modeling the impact of incidents and weather, as well as developing performance metrics for decision making purposes.

1.4 Outline of Report

The rest of the report is structured as follows. Chapter 2 summarizes literature on reliability performance analysis, incident and weather related modeling. Methodologies developed in this project, including secondary incident identification, IID quantification, and adverse weather impact analysis are presented in Chapter 3. Chapter 4 describes data sources used for the analysis and Chapter 5 presents the analysis results. Chapter 6 presents the conclusion of this study and recommendations for future research.

2.0 LITERATURE REVIEWS

2.1 Overview

In recent years the concept of data-driven performance evaluation has been gaining more and more popularity for traffic management. This chapter presents a literature summary on the three major components in this project: *performance metrics for reliability analysis*, *secondary incident identification and IID*, and *evaluation of adverse weather impact*.

2.2 Performance Metrics for Reliability Analysis

To quantify the roadway network performance, several standards are applied by the traffic operators. Travel time reliability has been widely used in different contexts to evaluate the performance of transportation facilities. In SHRP 2 L03 (2013), travel time reliability is defined as the level of consistency in travel conditions over time; while SHRP 2 L02 considers a system as reliable if each traveler's experienced actual time of arrival matches its desired time of arrival. Whichever definition is used, reliability is a critical measurement of congestion that users experience in a certain period of time. Various performance metrics are developed to describe travel time reliability, including Travel Time Index (TTI), Buffer Index (BI), Planning Time Index (PTI), Congestion Frequency, etc.

A number of previous studies have demonstrated the accuracy, sensitivity, and correlations of the above performance metrics (Edwards and Fontaine, 2012; Mahmassani, *et al.*, 2012; Mehran and Nakamura, 2009; Guo, *et al.*, 2012; Tu *et al.*, 2012). Table 2-1 shows a list of reliability measures examined in the previous work.

Table 2-1 Travel Time Reliability Measures from Previous Works

Travel Time Reliability Measure	Saberi and Bertini (2010)	Pu (2011)	Lyman and Bertini (2008)	Van Lint and Van Zuylen (2005)	Alvarez and Hadi (2012)
90^{th} or 95^{th} Percentile Travel Time		√	√		
Coefficient of Variation	√	√			
Travel Time Index	√	√	√		√
Buffer Index	√	√	√		√
Planning Time Index	√	√			√
Misery Index				√	√
Skew of travel time distribution		√			√
Width of travel time distribution				√	
Congestion Frequency	√	√			
Others		Failure rate			Failure-on-time

Alvarez and Hadi (2012), Saberi and Bertini (2010) investigated the sensitivity of various reliability metrics in response to the variation of parameters of travel time distributions. Pu (2011) examined a number of reliability metrics assuming a log-normal distribution of travel time. He pointed out that for heavily right-skewed travel time distribution, the BI is not appropriate unless it is computed on the basis of the median rather than the mean. Saberi and Bertini (2010) reviewed existing methods with which travel time reliability is measured, including TTI, BI, PI, and Congestion Frequency. By comparing different reliability metrics in given segments, they draw the conclusion that BI and coefficient of variation (standard deviation of travel time divided by mean travel time) have a high consistency among other measures. Also PI and Congestion Frequency appear to follow similar pattern.

Some researchers focused on developing new measures of travel time reliability to overcome the disadvantages of the existing ones (Emam and AI-Deek, 2006; Van Lint and Van Zuylen, 2005; Liu, *et al.*, 2007), e.g., the reliability is insensitive to the geographical locations, or the reliability is estimated as a constant while it varies by departure time. (Emam and AI-Deek, 2006) proposed a new travel time reliability performance metric. The travel time reliability $R(T)$ is in response to a well-defined reliability engineering function $\lambda(T)$, namely failure rate function. The relationship between the reliability and the failure rate function is expressed as $R(T) = e^{-\int_0^T \lambda(t)dt}$, where $\lambda(t) = f(t)/R(T)$ and $f(t)$ is the probability distribution function. Compared with existing methods, their new method emphasizes more on user's perception of

travel experience, and has strong potential in estimating travel time reliability as a function of departure time. Van Lint and Van Zuylen (2005) proposed two reliability metrics based on 10^{th}, 15^{th}, and 90^{th} precentile of the day-to-day travel time distribution for a given route based on Day-of-Week Time-of-Day (DOW- TOD) under the consideration that mean and variance tend to obscure important features of the reliability distribution under certain circumstances. They used skewness and width of travel time distribution as indicators. It is concluded that the metrics can effectively identify the unreliability of travel times for a given DOW-TOD period.

2.3 Secondary Incident Identification and Incident-Induced Delay

The challenge of IID quantification lies in the extraction of IID from the total delay, which is the result of compounding effect of recurrent and non-recurrent congestion. Recurrent delay is defined as congestion caused by routine traffic operation in a typical setting. Non-recurrent congestion is the unexpected or unusual congestion caused by an event that is transient relative to other similar days (Hallenbeck *et al.,* 2003). Seven sources are identified as potential sources for non-recurrent congestion by FHWA in SHRP 2. They are incidents, extreme weather, work zones, demand fluctuations, special events, traffic control devices, and inadequate base capacity. Kwon *et al.* (2006) found that congestion caused by incidents is 3 to 5 times of the ones caused by special events and weather. Also considering the fact that incident is more common than other unreliability sources, it is necessary to perform IID estimation in an effort to quantify the non-recurrent congestion impact.

Numerous studies have been conducted to quantify IID. Methodology-wise, three methods are most widely used, including deterministic queueing theory (Li, *et al.*, 2006; Wang, *et al.*, 2008; Runze Yu *et al.,* 2014), shockwave theory (Mongeot and Lesort, 2000; Chandana Wirasinghe, 1978), and statistic method (Skabardonis, *et al.*, 2003). Deterministic Queuing Theory (DQT) is implemented in the Highway Capacity Manual (HCM) for estimating delay. In DQT, delay is calculated as the area enclosed by the arrival and departure curves, requiring key parameters, such as arrival rate, departure rate, incident duration, and capacity, to be determined before the calculation. The parameters are either assumed or via stochastic method, and the estimation accuracy is compromised when applied to individual incident (Li, *et al.*, 2006). Some of the parameters are hard to be determined for predicting incident delay in dynamic networks.

Yu *et al.* (2014) proposed a modified DQT method and avoided the parameters estimation using short-term traffic flow forecasting. However, the method yields unsatisfying results when the incident happens during unstable traffic conditions (e.g. oversaturated condition downstream). Shockwave-based algorithms are developed on the basis of traffic flow theory, treating incidents as flow perturbations. The algorithm suffers from mathematical complications, and are difficult to be implemented within the existing performance measurement infrastructure. In Mongeot *et al.* (2000), the algorithms is fulfilled with first-order macroscopic traffic flow model. It is assumed in the study that the traffic flow is in equilibrium status constantly, which further ignored the speed and volume reduction due to the queuing phenomenon. Statistical models were also applied in the previous research to estimate congestion. Compared with the other two methods, it is easier to be implemented and has loose constraints on the quality of sensor data (Skabardonis, *et al.,* 2003). However, the methods are not capable of estimating the delay at microscopic level.

To quantify IID, one challenge is to rule out the impact induced by secondary incidents. Secondary incidents are considered as stochastic events induced by traffic congestion originated from the primary incident. A loose assumption regarding secondary incident identification is that secondary incidents happen within certain spatial and temporal range of primary incidents. To simplify the identification procedure, the majority of previous studies have used fixed spatial and temporal boundaries, assuming that the selected boundaries are applicable to all types of incidents. Khattak, *et al.* (2009) provides a summary on the previous work, most of which used spatial and temporal boundaries up to 2 miles and 120 minutes. Considering the fact that incident impact varies with the geometric characteristics of the road, periodic characteristics of traffic, and incident type, the general assumption of fixed spatiotemporal boundary lacks universality. To accommodate the varying spatiotemporal boundaries, Chung (2013) and Yang, *et al.*, (2013) presented data-driven dynamic methods to estimate primary incidents' impact based on traffic features and incident data.

Yang, *et al.* (2013) believed that one location is under the impact of previous incidents if the speed at this location is lower than the historical speed value. They thus constructed spatiotemporal binary speed plot of each incident by comparing the speed value against the historical incident-free speed profile at the same location. They also developed an algorithm to identify if the following incidents are within the spatiotemporal impact range of the previous

incident. Under ideal condition, the impact range demonstrates continuous stripe pattern stretching upstream spatially and downstream temporally. However, due to loop detector errors and bias in estimating incident-free speed, there are interrupting structures (bubbles) in the actual impact range (Chung, 2013). To eliminate the effects of the interrupting structures, they proposed three criteria for impact range identification: 1. the spatiotemporal progression of the incident shockwave is uninterrupted; 2. the boundary of the spatiotemporal progression of the incident shockwave is upstream; and 3. the entire boundary of the affected region is contiguous.

2.4 Evaluation of Adverse Weather Impact

Another major source for non-recurring congestion is adverse weather, which leads to changes in driver behavior that affect traffic flow. Many studies focused on the adverse weather's impact on crash occurrence and the overall traffic condition (Bergel-Hayat *et al.*, 2013; Yu *et al.*, 2013; El-basyouny *et al.*, 2014; Ahmed *et al.*, 2014; Brijs *et al.*, 2008). Yu *et al.* (2013) studied real-time weather's effect on crash frequency by adding seasonal weather related random factor to Bayesian random effect model. El-basyouny *et al.* (2014) investigated the impact of weather elements, especially sudden extreme snow or rain weather, on crash type using Bayesian multivariate Poisson lognormal model.

Numerous efforts have been performed by researchers to study weather's effects on traffic condition, e.g. traffic flow, speed, and non-recurrent congestion (Datla and Sharma, 2008; Maze et al., 2006; Thakuriah and Tilahun, 2012; Keay and Simmonds, 2005; Chung, 2012). Keay and Simmonds (2005) investigated the relationship between weather variables and traffic flow at different time-of-day by performing regression analysis. Chung (2012) used the spatiotemporal analysis to quantify the congestion caused by precipitation events.

2.5 Summary

This chapter summarized the key findings from the literature search for this study. Three main topics of focus in this project include performance metrics for reliability analysis, secondary incident identification and IID, and evaluation of adverse weather's impact. Previous studies have been focusing on addressing these issues with theoretical modeling and statistical methods. In the following chapters, we will present our data-driven solutions on these problems.

3.0 RESEARCH METHODS

3.1 Overview

To conduct data-driven performance evaluation on a freeway corridor, Traffic data with high resolution need to be collected to assist with the analysis. I-15 is chosen as the study corridor in this project. I-15 stretches 401.07 miles long in the State of Utah and connects the vast majority of the state's population and employment centers. For demonstration purpose, the corridor segment from MP 285 to MP 310 on I-15 Northbound is chosen to illustrate the performance analysis process. This segment lies in the Salt Lake City metropolitan area where the majority of accidents are observed, with 60 valid stations. Figure 3-1 is a map of the selected segment of the I-15 corridor. In the subsequent analysis, interpolation is applied for a finer time resolution need and for incidents that are located between stations.

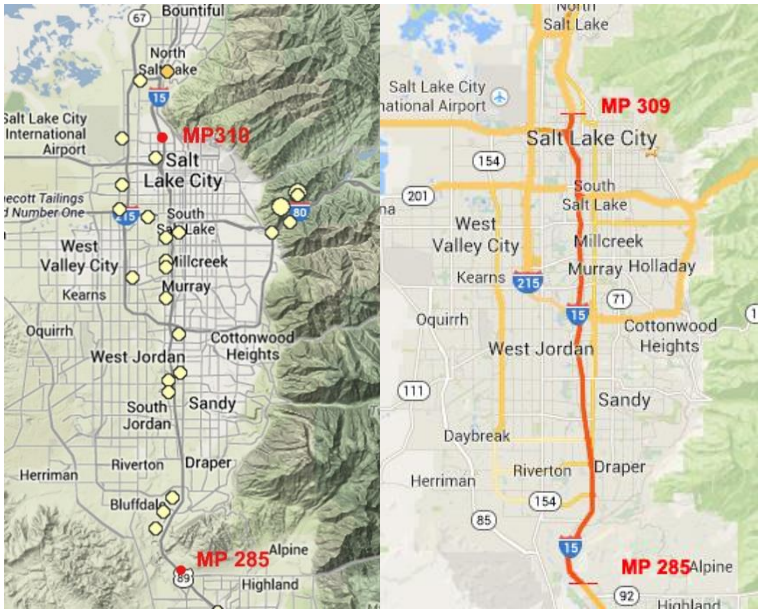

Figure 3-1 I-15 Study Corridor

3.2 Performance Metrics for Reliability Analysis

UDOT is currently using speed profile to describe the travel reliability along I-15 corridor. The speed measure (mean, 15th and 85th speed percentile) is intuitive and interpretative for both practitioners and the general public. Figure 3-2 displays this reliability measure along

the I-15 corridor. However, it would be desirable if a unified measure can be developed to describe the same speed variation, yet is easily comprehended. Congestion Frequency is recommended as a measure of reliability by FHWA. It is typically expressed as the percentage of days or time that travel times exceed X minutes or travel speeds fall below Y mph. It is relatively easy to compute given the availability of traffic data, and typically reported for weekdays during peak periods.

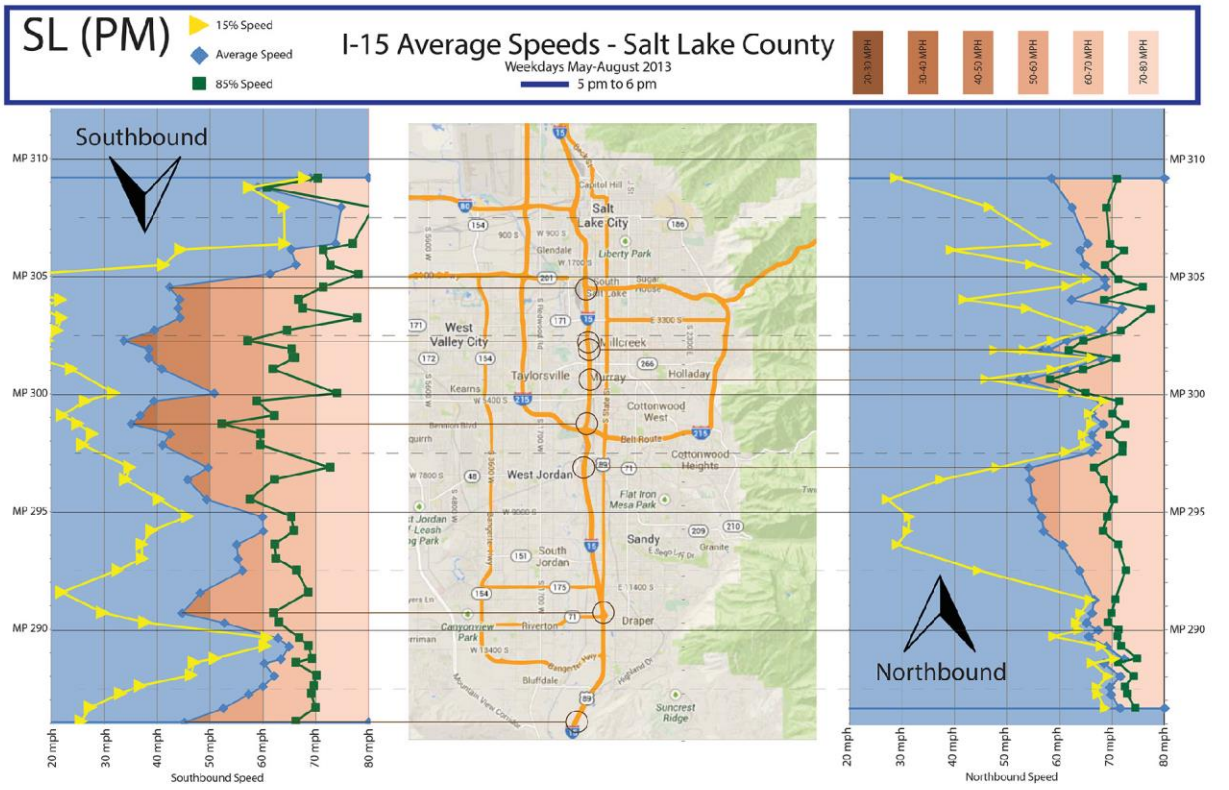

Figure 3-2 Speed Profile at 15th, 50th, and 85th Percentiles across Study Corridor

The speed threshold below which the roadway condition is considered congested is critical in congestion frequency measurement. In Pu's (2011) work, congestion is defined as the condition when speed is less than or equal to 50% of the free-flow speed, or equivalently, travel time is more than or equal to twice of the free-flow travel time. In Pu (2011), $Travel\ Time\ Index = 1.3$ is used as a criterion to define congestion. In this study, traffic breakdown (congestion criterion) is identified via speed-flow relationship along the I-15 corridor. Figure 3-3 shows the speed-flow scatter plot using the empirical data collected on I-15. Traffic breakdown occurs around 50-55 mph. Thus, 55 mph is adopted in this study as the speed

threshold in the Congestion Frequency measure. This is also consistent with Lyman and Bertini's (2008) definition, where using the average speed at midnight as the free-flow speed (69 mph on I-15), the speed threshold is estimated as 53 mph ($1.3 * FFS$).

Figure 3-4 shows the sensitivity analysis of the Congestion Frequency measure under different speed thresholds. The result of the analysis is illustrated as heat maps where the spatial and temporal pattern of Congestion Frequency can be observed. It is noted that at MP 292-293, it is congested during the entire morning peak hour. As the congestion threshold increases (from 30 mph to 55 mph), more and more regions are identified as congested.

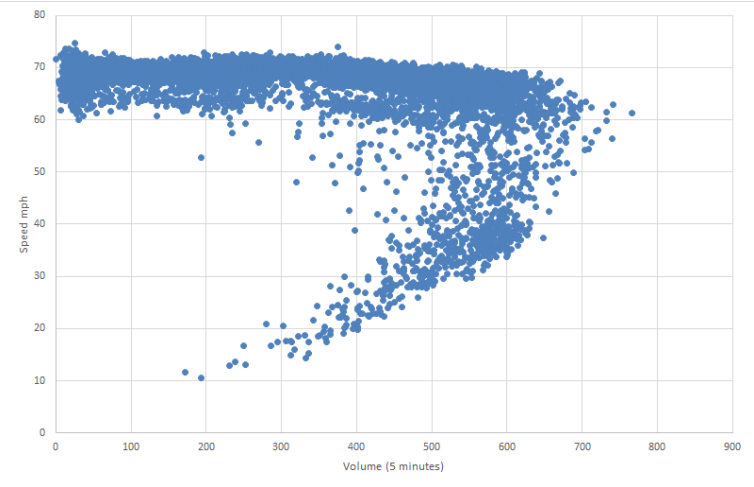

Figure 3-3 Speed-Flow Relationship using Empirical Data Collected

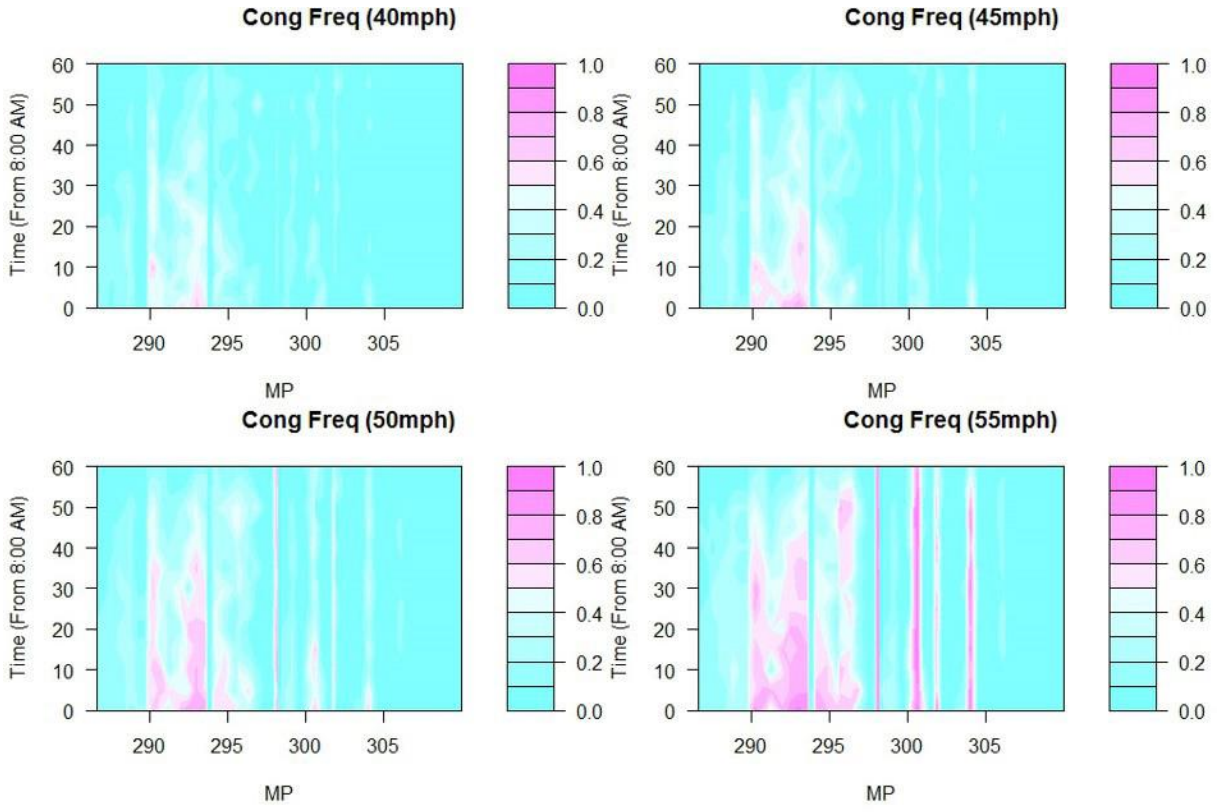

Figure 3-4 Congestion Frequency Heat Map under Different Speed Thresholds

3.3 IID

In this study, excess Vehicle-Hour Traveled (VHT) is employed as a measurement of traffic delay, defined as:

$$D = \Sigma F \times [TT - TT_t] = \Sigma F \times \max[\frac{L}{V} - \frac{L}{V_{ref}}, 0] \quad (1)$$

where *D* is the delay, TT is the travel time, TT_t is the travel time at threshold speed, L is the length of the segment, V is the speed, and V_{ref} is the threshold speed. The threshold speed is considered as the criteria for ideal travel experience.

The proposed methodology for IID estimation consists of three steps: 1. Secondary incident identification; 2. Spatial and temporal analysis of incident's impact extent; and 3. Pattern matching for recurrent congestion determination. The following subsections detail the implementation of the three steps. Figure 3-5 shows the flowchart for IID quantification procedure.

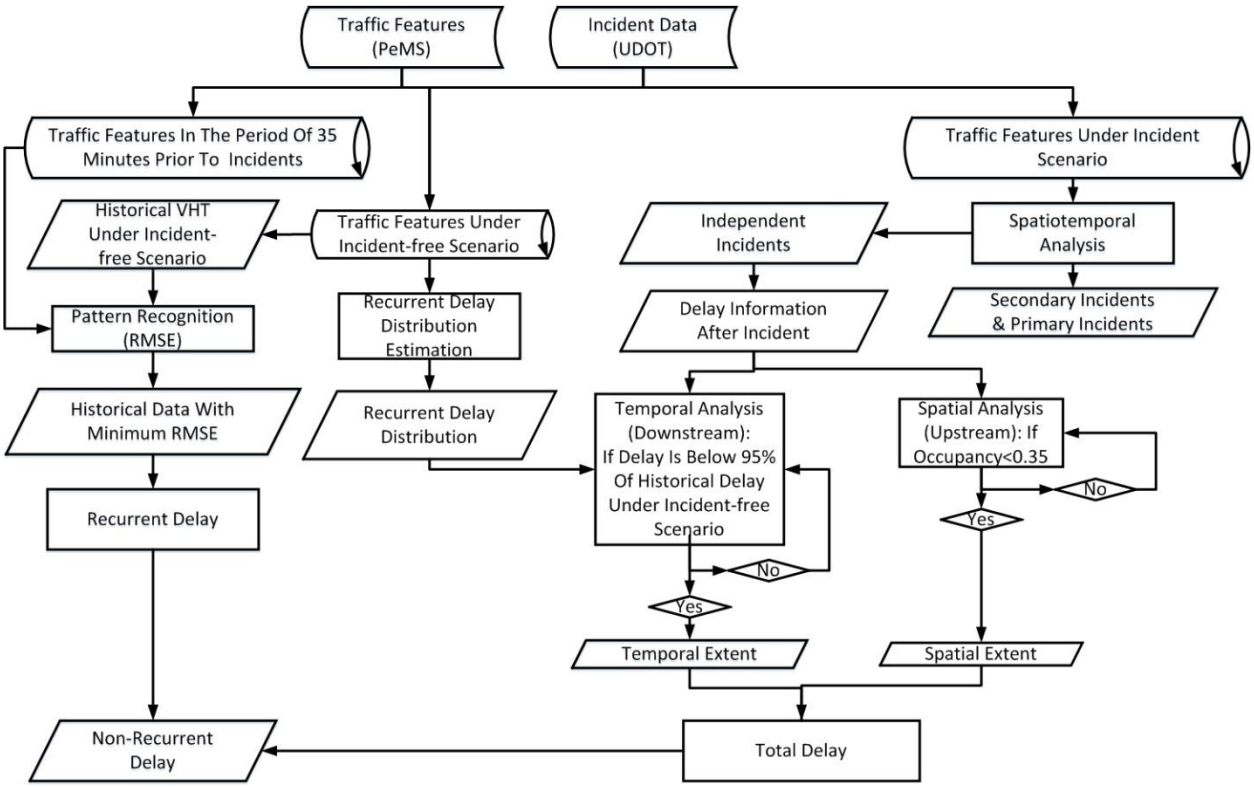

Figure 3-5 Flowchart of Incident-Induced Delay Estimation

3.3.1 Secondary incident Identification

The proposed methodology aims at identifying secondary incidents by first locating them in spatiotemporal context related to the corresponding primary incidents. Then data-driven algorithm is developed to heuristically search for each individual incident through binary contour plot, shockwave front localization and contiguous region identification to determine its "secondary" nature.

1. Spatiotemporal domain and resolution

To simplify the mapping procedure and reduce the computational complexity, a sufficient spatiotemporal extent for all incidents is pre-determined as computational window before mapping each incident. The spatiotemporal extent should be sufficiently large so that all the impacts of incidents are included within the extent. However, if the window is too large, it will increase the computational load significantly. Thus, a domain of proper size is required. Based on the empirical testing, a spatiotemporal domain of 10 miles by 5 hours is quite desirable. The selected domain assumes that the impact of any incident is cleared within 5 hours after an incident happening and stretches no longer than 10 miles upstream. Another important

characteristic of the computational domain determination is resolution. Based on the nature of congestion propagation and dissipation, a time resolution of 1 minute and spatial resolution of 0.02 mile is chosen to capture the incident impact evolvement. The grid size of the entire computational domain is thus 300×500.

2. Delay contour plot

In this study, excess VHT with a speed threshold of 60 mph is employed as the measurement of traffic delay. The impact region for each individual incident is visualized in a spatiotemporal delay contour plot. Figure 3-6(a) shows a sample of the plot for MP305 on July, 15, 2013. The x- and y- axes refer to time and milepost, separately. The origin (top left corner) of the contour plot is the spatiotemporal location where the incident happened. In the spatiotemporal delay contour plot, the congested region, due to the total delay introduced by the traffic and incident, can be easily recognized. The total delay at cell (i, j) is represented by $D_{Sec}(i, j)$ in the delay contour plot, where *i* is the milepost of the location and *j* is the time stamp.

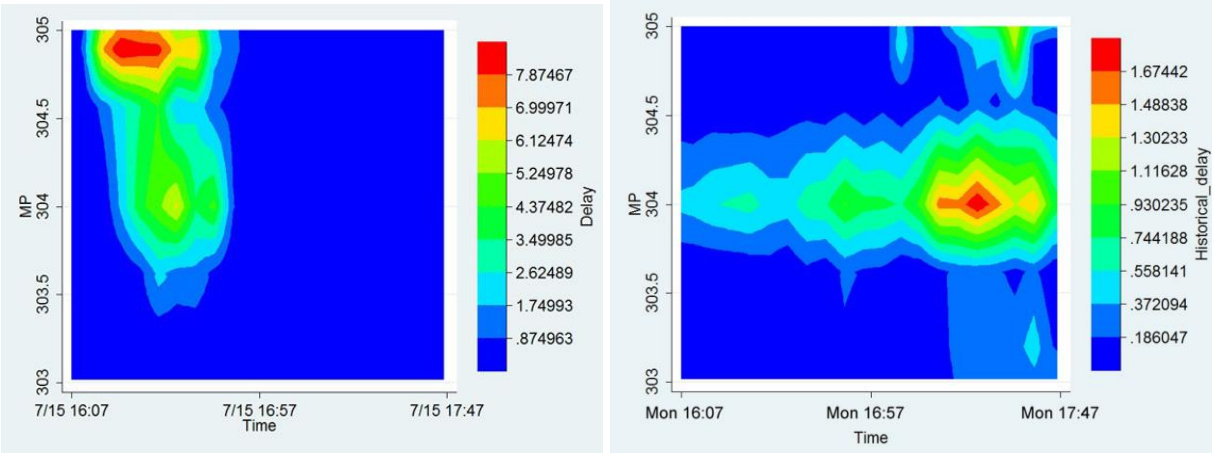

(a) Total delay for incident scenario (b) Historical delay contour plot

Figure 3-6 Example of Incident's Impact at MP 305 on July, 15, 2013

3. Historical delay contour plot

Let $d_{Sec}(i, j, k)$ be the representative of historical delay at MP i, time j, and week k. The delay under incident-free scenarios at MP i and time j but from different weeks $(d_{Sec}(i, j, 1), d_{Sec}(i, j, 2), \dots, d_{Sec}(i, j, n))$ follows certain distribution. The term *incident-free scenario* is defined as there is no incident happening within 5 hours prior to the time stamp nor within 10 miles upstream of the location. And the 80^{th} percentile of historical delays under incident-free scenario is used as the threshold to determine recurrent congestion. That is to say,

as long as the total delay is below the 80th percentile of historical delay, it is believed to be resulted from recurrent congestion. Figure 3-6(b) shows the sample historical delay contour plot.

4. Binary delay contour plot

By comparing the delay with the 80th percentile of historical delay, a binary contour plot can be generated for each incident. For cell (i,j), if the total delay $D_{Sec}(i,j)$ is higher than the 80th percentile of historical delay d_{ij}, the corresponding cell in the binary contour plot is marked as $I_{Sec}(i,j) = 1$, otherwise it is marked as $I_{Sec}(i,j) = 0$.

5. Shockwave front determination

One of the challenges in identifying the incident impact region is to determine whether the non-recurrent delay is caused by the incident or is induced by the biased estimation of the delay distribution. As a validation/calibration process, shockwave theory is applied in our method to determine the true effect of congestion and queuing induced by the incident. Once an incident occurs, the shockwave effect will take place. Thus, the incident impact region should coincide with the shockwave front, where only the cells behind the shockwave front are impacted by the incident. Recent studies on shockwave spreading proposed different methods to explore the shockwave front speed. In our study, we use a method proposed by Yang and Recker (2005) for estimating the position of the traffic shockwave front. The shockwave front is defined as the location where the vehicle density is greater than twice of the density upstream and average speed is greater than twice of the speed downstream.

6. Contiguous impact range

Given the fact that an incident's impact extends both temporally downstream and spatially upstream, the cells valid for a secondary incident must meet four criteria: 1. in the binary delay contour plot, cell (i,j) has $I_{Sec}(i,j) = 1$; 2. the cell is behind the shockwave front; 3. the cell is connected with the origin cell, where the primary incident happened; and 4. the temporally upstream or spatially downstream cell is impacted by the incident. These criteria are expressed as follows:

$$\begin{cases} I_{Sec}(i,j) = 1 \;\forall\, i \in (1,2 \ldots maximum\ time\ extent), \\ S(i) > j \\ C_{Sec}\big((i,j),(0,0)\big) = \max\Big(C_{Sec}\big((i-1,j),(0,0)\big) \times I_{Sec}(i-1,j), C_{Sec}\big((i,j-1),(0,0)\big) \times I_{Sec}(i,j-1)\Big) \\ = 1 \end{cases} \tag{2}$$

where $C\big((i_1, j_1), (i_2, j_2)\big)$ is the connection between (i_1, j_1) and (i_2, j_2). When the two cells (i_1, j_1) and (i_2, j_2) are connected, $C((i_1, j_1), (i_2, j_2))$ is equal to 1, otherwise 0. And $S(i)$ is the location of shockwave front at time i. If the incident happened in a cell satisfying all these criteria, it is considered as a secondary incident. Figure 3-7 shows an example of the primary and secondary incident matching.

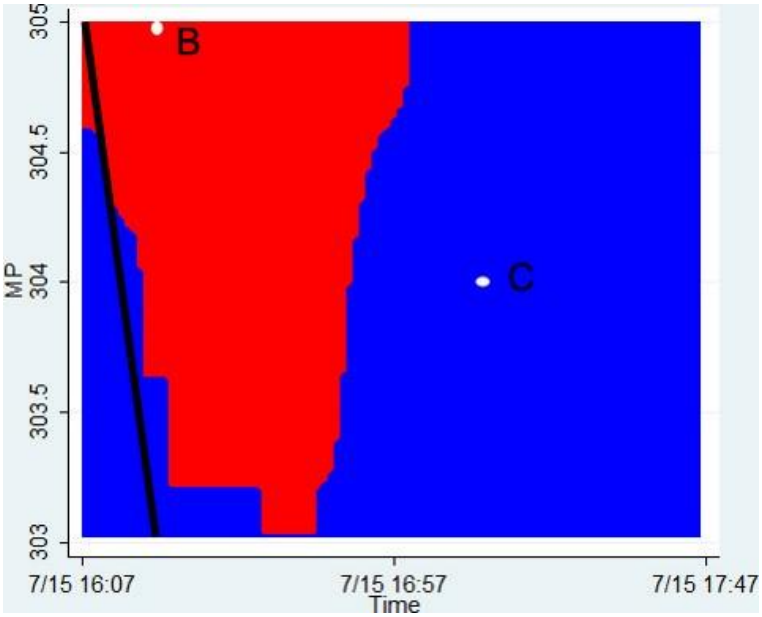

Figure 3-7 Example of Primary and Secondary Incident Matching

3.3.2 Spatial and temporal analysis for incident's impact extent

The threshold speed of 60 mph is determined using the analytical approach by Van Aerde's to model the speed-flow relationship from the empirical data collected on I-15. Van Aerde's steady-state speed-flow model is a multivariate estimation procedure that can determine capacity, free-flow speed, speed at capacity, and jam-density via iterative numerical search (Van Aerde and Rakha, 1995). Figure 3-8 shows the speed-flow plot with the Van Aerde's curve fitting. Note that the speed at capacity is determined as 60 mph, which is used as a threshold to distinguish between free-flow and congested regimes.

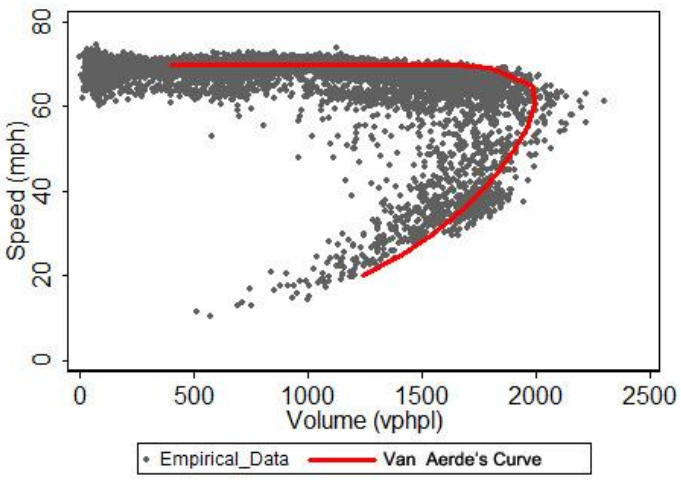

Figure 3-8 Speed-Flow Plot with Van Aerde's Curve Fitting

To assist with the IID estimation, the relational traffic databases are divided into three sections: 1. Traffic data across the incident duration and 30 minutes after the incident ends; 2. Traffic data for the incident-free scenario (same location, DOW-TOD with the incident); and 3. Traffic data 30 minutes prior to the incident happening. The incident-free scenario is defined as, in spatial and temporal domains, no incident 30 minutes prior to the scenario, and no incident within 8 miles of the location during peak hour and 3 miles during non-peak hour. The spatiotemporal extent for the incident-free scenario is capable of excluding almost all the incident's impact, which was concluded from the primary and secondary incident's delay contour plots.

When an incident happens, total delay is accumulated from the moment that the incident occurs until the moment that its impact is totally cleared. Most of the time, the incident impact clearance time is longer than the incident clearance time. And under congested conditions, the difference would be even more pronounced. It is thus not feasible to treat incident clearance time as the time stamp that the IID ends. In this study, regression analysis is applied to determine the impact clearance time. If an incident brought extra delay to the traffic, the delay at the moment when the incident was cleared should be higher than the delay for the typical incident-free scenario at the same location and time stamp. It is assumed that the incident's impact is not cleared until the delay falls within an acceptable range of the historical incident-free data. To achieve this, we collected the one-year delay data at the incident end time for each individual incident. The distribution of this delay is then representative of the incident-free conditions.

To explain the distribution estimation procedure, a new variable I_{Inc} is introduced and defined as:

$$I_{Inc}(m,t,s,w) = \begin{cases} 1, & if\ the\ combination\ of\ (m,t,s,w)\ is\ incident-free \\ 0, & if\ the\ combination\ of\ (m,t,s,w) is\ not\ incident-free \end{cases} \quad (3)$$

where m is the location, t is the time, s is the DOW, and w is the week. $I_{Inc}(m,t,s,w)$ denotes whether the location m at the combination of time (t,s,w) is incident-free.

The estimation of incident-free delay can be expressed as

$$\widehat{D}_{Incf}(m,t,s,w) = \begin{cases} d_{Inc}(m,t,s,\mathrm{w}), if\ I_{Inc}(m,t,d,\mathrm{w}) = 1 \\ \widehat{D}(m,t,s,w), if\ I_{Inc}(m,t,d,\mathrm{w}) = 0 \end{cases} \quad (4)$$

Where $d_{Inc}(m,t,s,w)$ is the historical delay at the temporal and spatial combination of (m,t,s,w), $\widehat{D}_{Incf}(m,t,d,w)$ is the estimation of delay at (m,t,s,w). When $I_{Inc}(m,t,s,w) = 1$, the traffic is in incident-free status, so the estimation of delay is equal to historical delay. If $I_{Inc}(m,t,s,w) = 0$, the delay is estimated from other incident-free scenarios at the same location and DOW-TOD.

The incident-free delay distribution demonstrates a pattern that follows Weibull distribution $f(x;\lambda,k) = \frac{k}{\lambda}\left(\frac{x}{\lambda}\right)^{k-1} e^{\left(-\frac{x}{\lambda}\right)^k}$ $(x \geq 0)$, with shape parameter of $k = 1$ or $k = 2$. Figure 3-9 presents three typical histogram plots that match Weibull distribution with (1) $k = 1$; (2) $\mathrm{k} = 2$; and (3) no statistical characteristics observed, separately. Cases without obvious statistical characterization all happened at MP 304 during 16:00 to 18:00 on Saturday. Since the delays during this time period at MP 304 are unpredictable, these incidents were excluded. Based on this finding, estimation of Weibull distribution regarding different shape parameters were performed. When $k = 1$, Weibull distribution is equivalent to Exponential distribution. The probability density function is $f(x;\lambda) = \lambda e^{-\lambda x}$ $(x \geq 0)$, and cumulative distribution function is $F(x;\lambda) = 1 - e^{\lambda x}$ $(x \geq 0)$. The parameter λ is estimated with $\hat{\lambda} = \frac{n}{\Sigma_{i=1}^{n} x_i}$. When $k = 2$, Weibull distribution is equivalent to Rayleigh distribution. The probability density function i $f(x;\sigma) = \frac{x}{\sigma^2} e^{-\frac{x^2}{2\sigma^2}}$ $(x \geq 0)$ s, and cumulative distribution function is $F(x) = 1 - e^{-\frac{x^2}{2\sigma^2}}$ $(x \geq 0)$. The parameter σ is estimated using $\hat{\sigma} = \sqrt{\frac{1}{2n}\Sigma_{i=1}^{n} x_i^2}$. The incident impact clearance time is thus

determined as the moment when the delay falls into the lower 5% tail of the incident-free delay distribution. Thus, for Exponential distribution:

$$F(x;\lambda) = 0.05 \rightarrow x_{exp} = \frac{ln1.05}{n}\Sigma_{i=1}^{n} x_i \tag{5}$$

For Rayleigh distribution:

$$F(x;\sigma) = 0.05 \rightarrow x_{Ray} = \sqrt{\frac{ln1.05}{n}\Sigma_{i=1}^{n} x_i^2} \tag{6}$$

It is assumed that delay pattern follows the regular trends afterwards as soon as it is below the minimal value of $x_{exp}$and x_{Ray}.

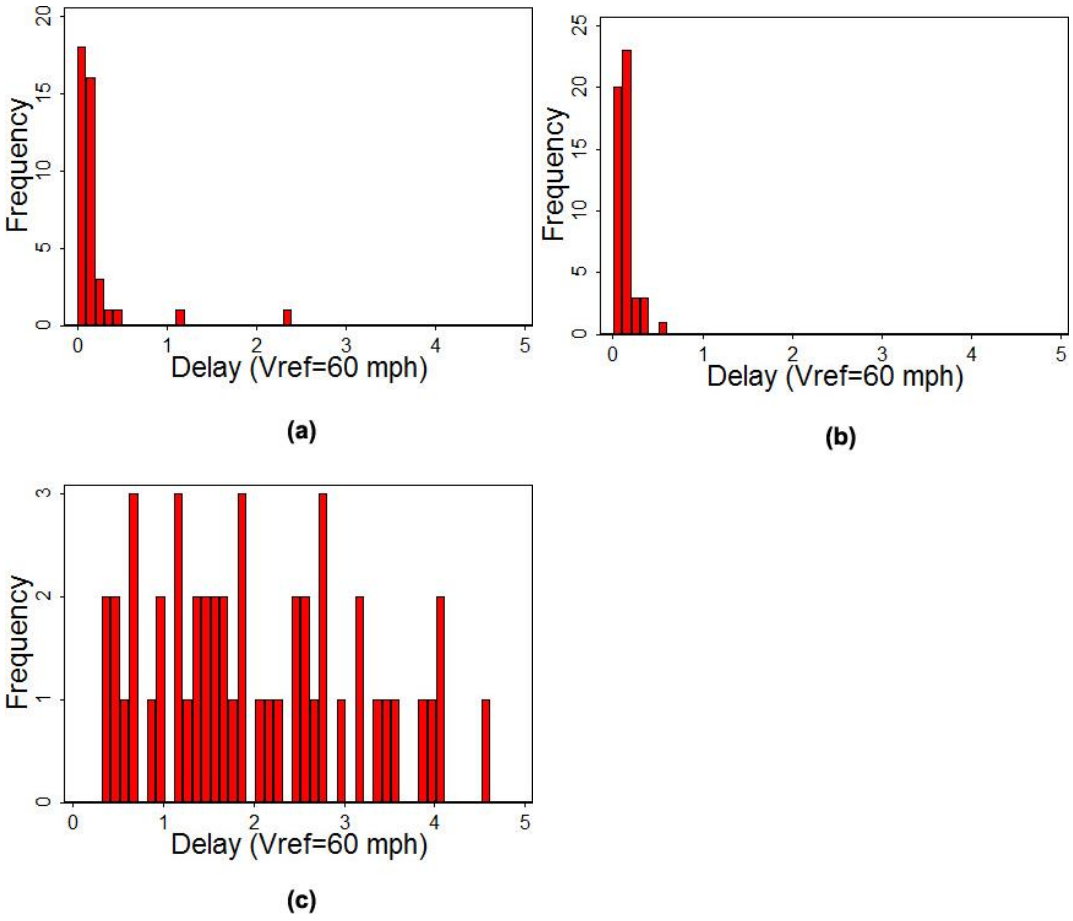

Figure 3-9 Sample Delay Histogram for Incident-Free Scenario

After identifying the temporal range of incident impact, the question follows to determine the spatial extents. Occupancy is used as a criterion to determine if the upstream location has a

queue formed. When the occupancy is greater than 0.35, it is considered that the traffic is in stop-and-go condition, thus the incident's impact has extended to the second nearest upstream station.

There are 60 stations $M_1, M_2, \dots, M_{60}$ in the selected I-15 segment. Assume Incident k happening at (m, t_{k1}, d, w), and the impact being cleared at time t_{k2}. The closest upstream station of location m is M_i. If the occupancy at M_i is greater than 0.35, it means that station M_i is congested and the delay at M_i should be included in the total delay. Then the algorithm will check the upstream stations $M_{i-1}, M_{i-2}, \dots, M_j$ subsequently, until the occupancy at M_j falls below 0.35. Then the accumulated delay from station M_{j+1} to the location where the incident happened throughout the incident duration is the total delay.

$$D_{Inc}(k) = \sum_{t_{k1} \le t_n \le t_{k2}} \left(\sum_{j+1 \le l \le i} d_{Inc}(M_l, t_n, s, w) + d_{Inc}(m, t_n, s, w) \right) \tag{7}$$

3.3.3 Pattern matching to determine the recurrent congestion delay

To determine IID for each individual incident, the challenge is to distinguish recurrent delay from total delay. In this study, we use a pattern matching method to identify the closest scenario (both spatially and temporally) from historical incident-free database, such that the recurrent delay can be estimated. VHT is used as the measure for the pattern matching, and Root-mean-square error (RMSE) is applied to find the most similar VHT pattern. RMSE is a widely used method for the quantification of the difference between observed values and estimated value:

$$\mathrm{RMSE}(\hat{\theta}) = \sqrt{\frac{\Sigma_{t=1}^{2}(\hat{y}_t - y_t)^2}{n}} \tag{8}$$

where n is the number of observations, $\hat{y}_t$ is the estimated value, and y_t is the observed value.

For each incident, seven VHT data points prior to the incident start time, which is equivalent to a time span of 30 minutes, are chosen to be compared with historical data via heuristic search for the same location, time-of-day, and day-of-week. The incident-free case with least RMSE would be recognized as a matching scenario and the delay occurred on that matching case across the incident duration would be treated as the recurrent delay during the incident. It is reasonable that some cases might have large RMSE due to the limited incident-free database and rare incident situation. Traffic condition is identified by volume and speed, and VHT is chosen as the variable that can reduce the complexity of pattern matching algorithm yet

represent the traffic condition. After filtering out holidays and overlapping incident scenarios, each incident has approximately 30-50 patterns from regular day to choose from. Figure 3-10 shows four sample pattern matching results for Incident No. 306, 502, 1179 and 1375, separately. Using Incident 525 as an example, it happened at 15:40 on 7/18/2013 at MP 286. There were 46 incident-free DOW-TOD patterns found in 2013. RMSEs of these 46 days range from 0.019 to 0.125. The least RMSE 0.019 occurred on 8/13/2013, and is chosen to be the matched pattern for calculating recurrent delay.

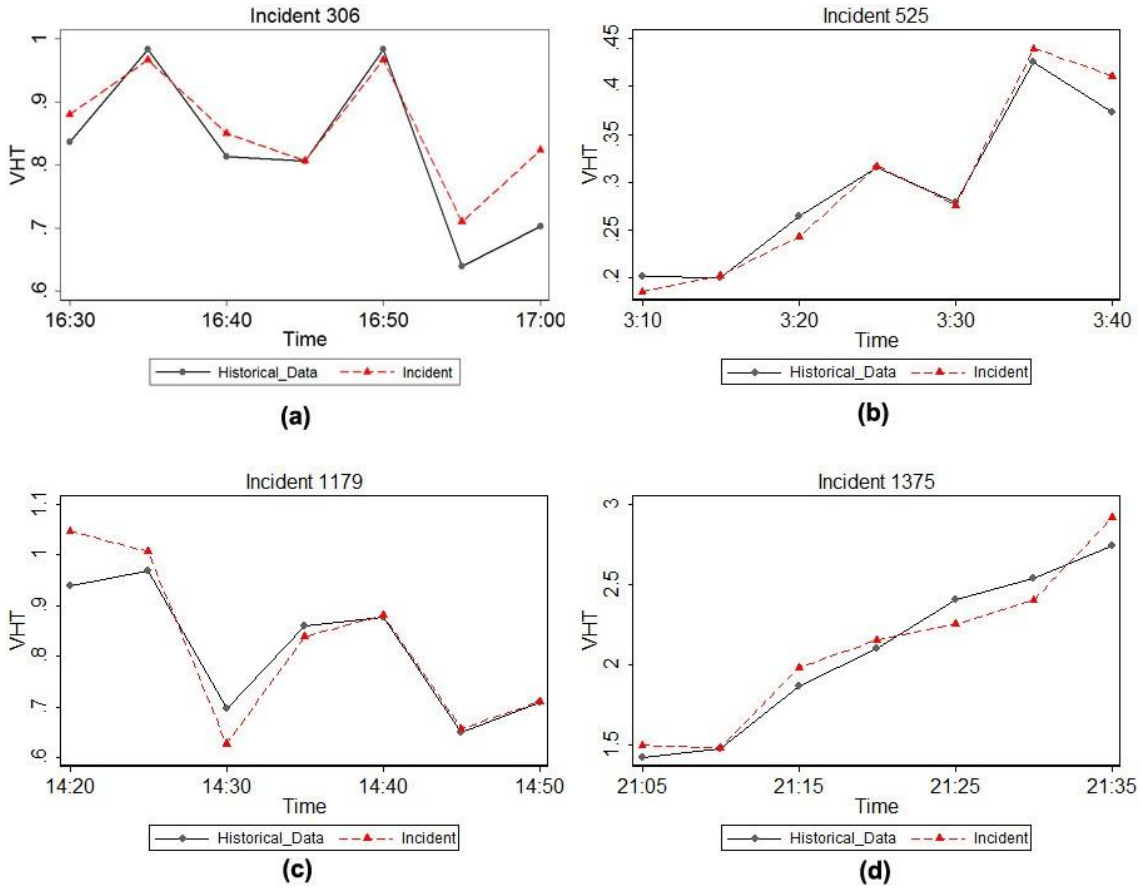

Figure 3-10 Examples of VHT Pattern Matching

Rather than using short-term prediction method, it is assumed the delay that occurred during the matching scenario is the recurrent delay when the incident happened. The recurrent delay during incident k is cumulated in the same spatial and temporal intervals as total delay. Assume that the matching incident-free time period is in week w_{his}, then the recurrent delay is calculated as:

$$D_{rec}(k) = \sum_{t_{k1} \le t_n \le t_{k2}} \left(\sum_{j+1 \le l \le i} \widehat{D}_{Infc}(M_l, t_n, s, w_{his}) + \widehat{D}_{Incf}(m, t_n, s, w_{his}) \right) \quad (9)$$

where all the variables have the same definitions as in Equation 6.

3.4 Evaluation of Adverse Weather's Impact

In this project, weather impact on traffic condition along the freeway corridor is examined. Although traffic condition degradation under adverse weather was observed in numerous studies, there is no study performed so far to quantitatively explore the relationship between adverse weather and degraded traffic conditions, which may be caused by many reasons (e.g. slippery road surface, vehicle performance degrade, and impaired visibility). Of particular interest of this study is the interaction between weather and delay. It is common that during adverse weather, people tend to rearrange or cancel their trips to avoid suffering longer travel time or taking higher risk of incidents. Since it is almost impossible to measure the actual demand along a corridor, we developed a mechanism to model the impact of adverse weather on throughput and delay.

To measure adverse weather impact on throughput and delay, historical traffic data (volume and delay) are retrieved from PeMS at the same DOW-TOD at the same location for each weather record. Data filtering process ensures that the historical records under the impact of incidents are ruled out. Let $\mathrm{D_{Wea}}(m, t, s, w)$ be the delay when the adverse weather is reported, where m is the location, t is the TOD, d is the DOW, and w is the week. The historical delay at the same location and time stamp is represented using $d_{Wea}(m, t, s, u)$, where $u = 1,2, \dots, 54$, $u \neq w$, and $I_{Inc}(m, t, s, u) = I_{Inc}(m, t, d, w) = 0$. The same data retrieval is performed on throughput (volume), and $F_{Wea}(m, t, s, w)$ and $f_{Wea}(m, t, s, u)$ represent the flows under adverse weather and historical normal days, separately. For the historical delay records, if the flow difference (under normal day vs. adverse weather day) falls below certain threshold, then the delay under the normal day is counted as one of the sample representative for further analysis. This can be expressed as:

$$\widehat{\mathrm{D}}_{\mathrm{Weaf}}(m, t, s, w) = \frac{1}{\mathrm{n}} \Sigma_{\mathrm{i}=1}^{\mathrm{n}} d_{Wea}(m, t, s, u_i), \quad if \ \left(abs\left(F_{wea}(m, t, s, w) - f_{Wea}(m, t, s, u_i)\right) \le \text{Flow Threshold}\right) \quad (10)$$

The threshold is chosen as 10% of the values during the adverse weather. Similarly, for the historical flow records, if the delay difference (between normal day vs. adverse weather day) falls below a certain threshold, the flow under the normal day is counted as one of the sample representative for further analysis:

$$\hat{F}_{Weaf}(m,t,s,w) = \frac{1}{n}\Sigma_{i=1}^{n} f_{Wea}(m,t,s,u_i), \quad if\ \left(abs\left(D_{wea}(m,t,s,w) - d_{Wea}(m,t,s,u_i)\right)\right) \leq \text{Delay Threshold} \tag{11}$$

Subsequently $\Delta \mathrm{D}_{\mathrm{wea}}(m,t,s,w)$ and $\Delta \mathrm{F}_{\mathrm{wea}}(m,t,s,w)$ can be calculated to quantitatively measure the impact of adverse weather on delay and traffic throughput, where:

$$\Delta \mathrm{F}_{\mathrm{wea}}(m,t,s,w) = \hat{F}_{Weaf}(m,t,s,w) - F_{wea}(m,t,s,w) \tag{12}$$

$$\Delta \mathrm{D}_{\mathrm{wea}}(m,t,s,w) = \hat{D}_{Weaf}(m,t,s,w) - D_{wea}(m,t,s,w) \tag{13}$$

3.5 Summary

In the chapter, the methodologies for reliability analysis, IID and secondary incident identification, and weather impact evaluation are presented. Congestion frequency is considered as a comparable measure to the speed percentile for describing freeway reliability yet is easy to interpret. The IID and secondary incident identification adopt spatiotemporal analysis at individual incident level and heuristically search from the historical traffic database to match the recurrent delay. A simplified estimator is developed to model the weather impact in terms of traffic volume and delay. In the following chapters, the methodologies developed will be applied to the data collected through PeMS, incident and weather databases to demonstrate the performance evaluation result.

4.0 DATA COLLECTION

All the traffic data used in this project are from PeMS (Freeway Performance Measurement System), hosted and managed by Iteris in the Cloud. It is designed to collect, filter, process, aggregate, and examine traffic data provided by UDOT. The system contains a rich pool of information about real-time and historical traffic data and provides an excellent platform to both transportation practitioners and researchers. The system integrates various traffic data sources including loop detectors, incident logs, vehicle classification data, and roadway inventory, etc. These traffic data have been automatically collected and archived from over 28,000 detectors every 30 seconds, which totals 46 billion data samples per year. Meanwhile, UDOT maintains separate databases for vehicle incident tracking in TOC. These datasets offer details regarding incident ID, time, location, duration, severity, priority, impact, and brief description. For IID and secondary incident identification, we obtained the incident database for the year 2013 with 9,302 incident records. And 1,377 of them are used for modeling purpose since they occurred along I-15 Northbound between MP 285 to 309. The weather data used in this project are obtained from the Traveler Advisory Telephone System (TATS) database. These data were collected by trained citizen reporters, who can be UDOT employees, law enforcement, truck drivers, plow drivers, experienced commuters, or other volunteers, to report on the current road conditions along specific segments across Utah. We obtained the dataset from November 2013 to March 2014, including road condition, sky condition, date and time, reporter, and route segment ID. There are more than 190,000 records on freeways and arterials throughout the State, and more than 3,000 records on the selected corridor in the Salt Lake Metropolitan Area. The weather data is categorized by road condition as dry, wet, slushy, patchy snow, icy spots, and snow covered, and by sky condition as rain, mixed rain and snow, blowing snow, and snow.

5.0 DATA ANALYSIS

5.1 Overview

In this Chapter, we will apply the methodologies presented in Chapter 3 to the data collected in the State of Utah. The analysis shows the performance evaluation at both corridor level and location level. The results demonstrate strong policy implications that will potentially lead to the incorporation of the measures/algorithms into the roadway traffic management and assist with project prioritization.

5.2 Performance Metrics for Reliability Analysis

Congestion frequency is computed using traffic condition data in 2013 with 55 mph as the threshold for this I-15 study corridor. Figure 5-1 shows the congestion frequency and speed profile along I-15 for morning and afternoon peak hours. It is shown that the two measures demonstrate a consistent pattern. Congestion frequency is in the range of 0 to 1 and can be translated into the probability that the travelers will experience certain traffic condition. A congestion frequency of 1 suggests that if the user drives to the location during that time period, he/she will be sure to experience a speed less than 55 mph. It is shown from Figure 5-1 that during morning peak hour there is a high probability of speed less than 55 mph at MP 290 and MP 301 on Northbound I-15, and at MP 301 and MP 309 on Southbound I-15. During evening peak hour, there is a high probability of speed less than 55 mph at MP 296 and MP 309 on Northbound I-15, and at MP 286, MP 301, and MP 304 on Southbound I-15.

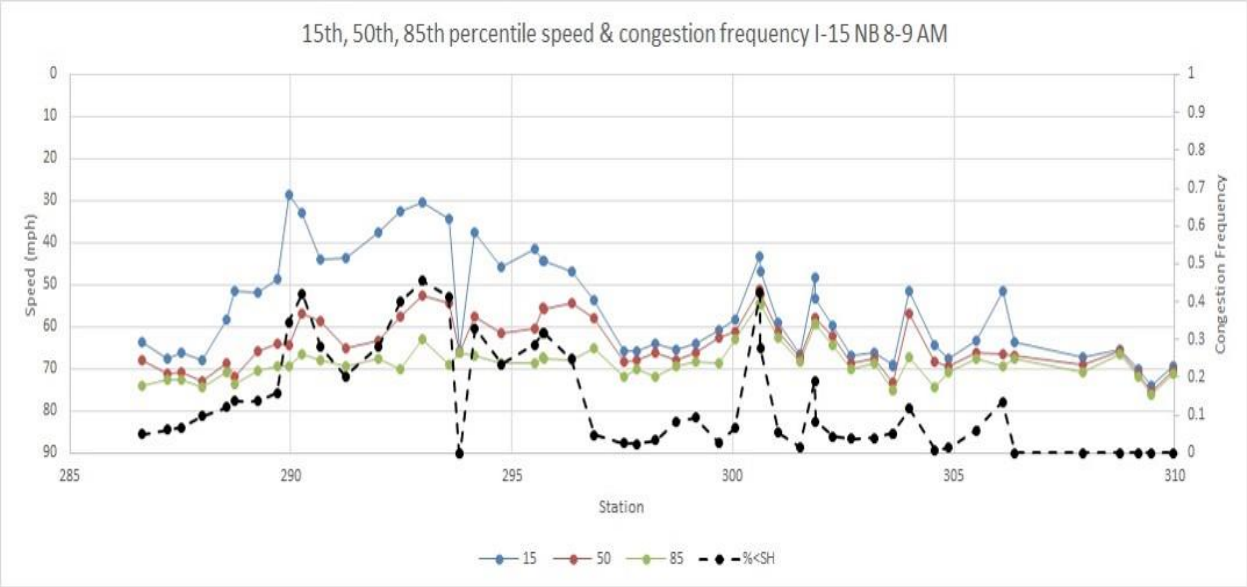
15th, 50th, 85th percentile speed & congestion frequency I-15 NB 8-9 AM
Speed (mph)
Congestion Frequency
Station
15
50
85
%<SH

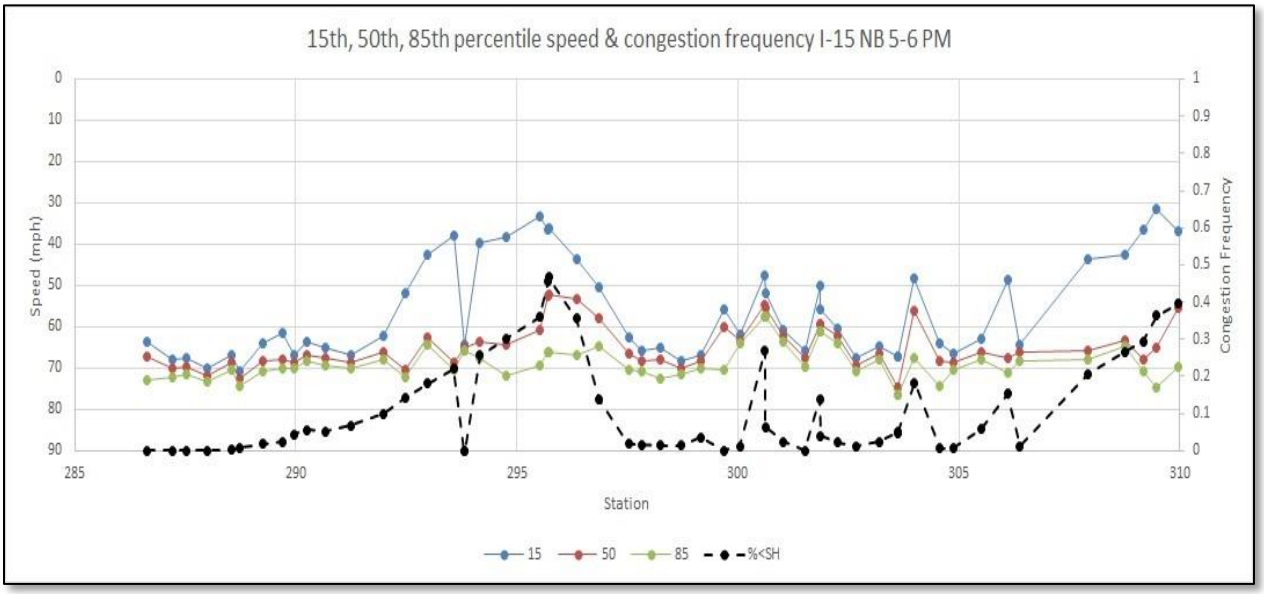
15th, 50th, 85th percentile speed & congestion frequency I-15 NB 5-6 PM
Speed (mph)
Congestion Frequency
Station
15
50
85
%<SH

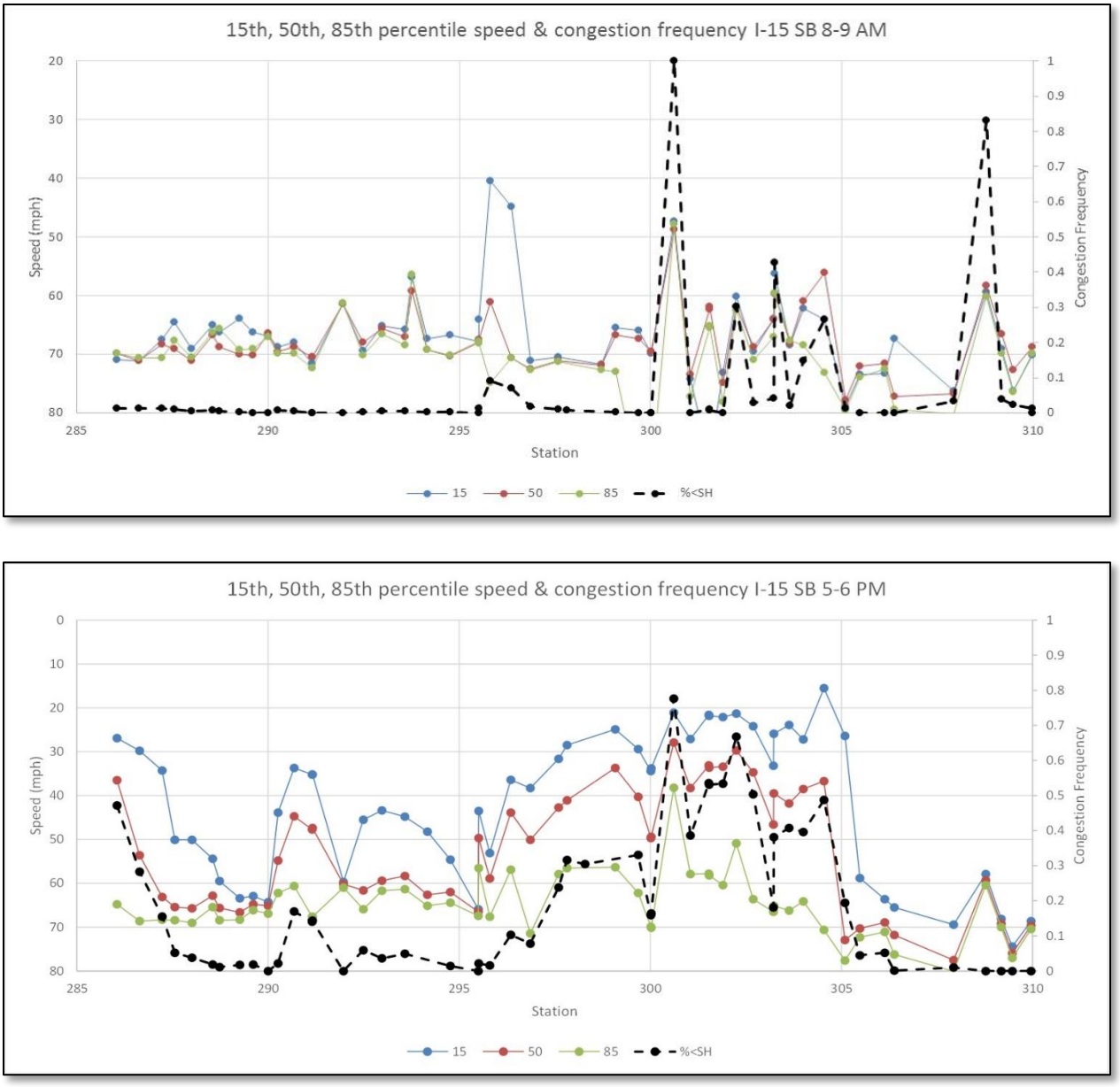

Figure 5-1 Congestion Frequency and Speed Profile at 15th, 50th, and 85th Percentiles across I-15 Study Corridor

5.3 Secondary Incident Identification

Applying the data-driven algorithm described in Section 3.3.1 to the 2013 incident database, we identified 240 secondary incidents as a result of 109 (7% of the total incidents)

primary incidents along the I-15 northbound study corridor during year 2013.

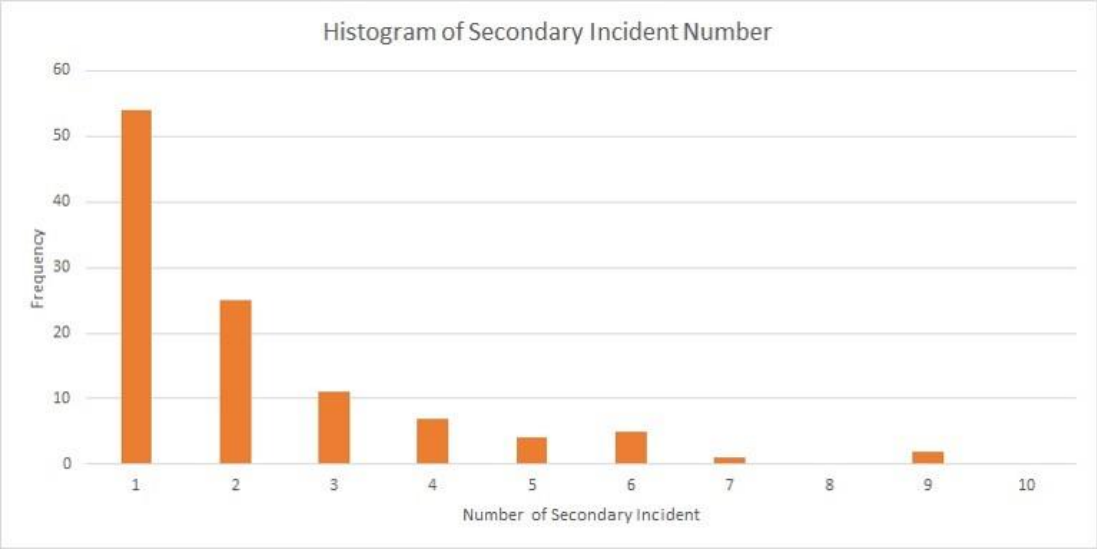

shows the histogram of number of secondary incidents caused by each primary incident. Figure 5-3 shows the distribution of secondary incidents by month. The distribution demonstrates a pronounced seasonal pattern, with December having the most secondary incidents. This implies that precipitation and slippery road conditions increase the probability of secondary incident occurrence.

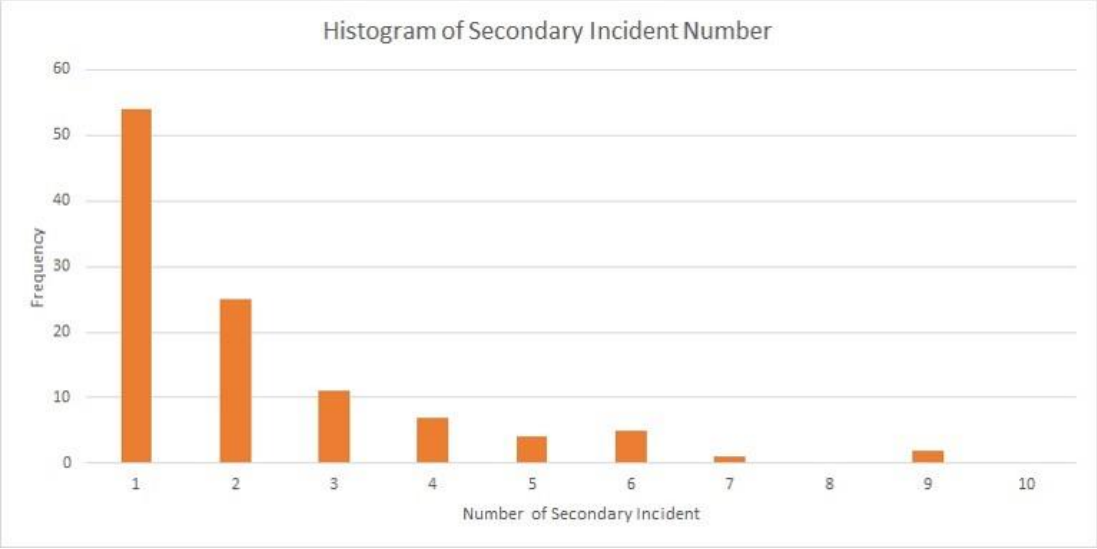

Figure 5-2 Histogram of Secondary Incident Induced

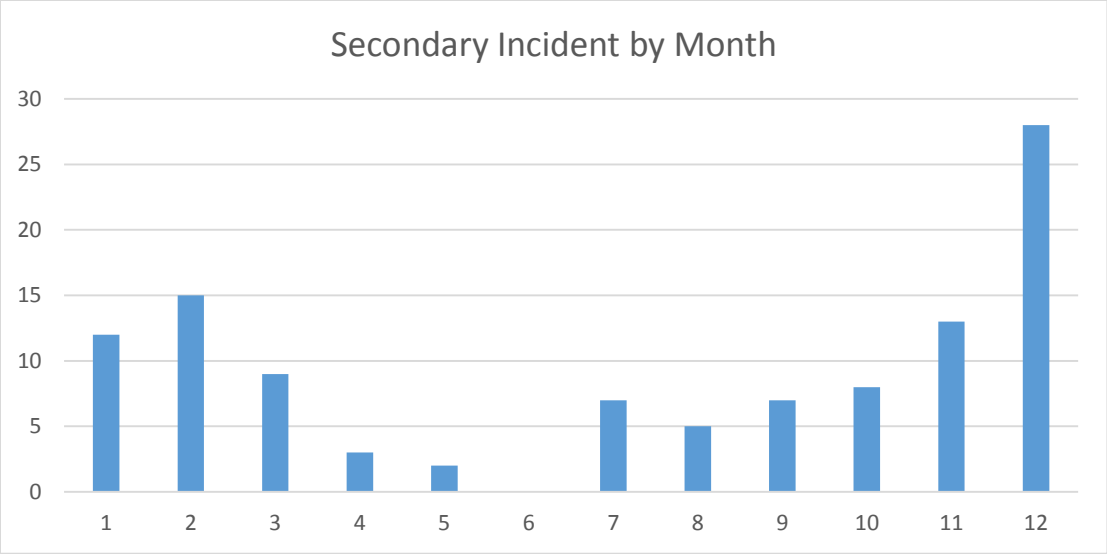

Figure 5-3 Secondary Incident Distribution by Month

5.4 IID

The incident records provided by TOC contain additional information besides the location and duration of the incidents, including incident priority, impact and severity. The definitions of these variables are shown in Table 5-1.

Table 5-1 Operator's Estimation of Incident Information

Level		From Low to High			
Priority	Value	1	2	3	4
	Meaning	No blocking lane	Less than 1/2 of total lanes blocked	Greater than 1/2 of total lanes blocked	All lanes closed
Severity	Value	None	Low	Medium	High
	Meaning	No property damage	Fender bender	People injury and property damage	Fatality, Multiple PI, PD, hazmat, major event
Impact	Value	1-3	4-6	7-10	
	Meaning	Less than 5 min	5-15 min	Greater than 15 minutes	

Operators' estimation of incidents is quite intuitive and sometimes inaccurate.

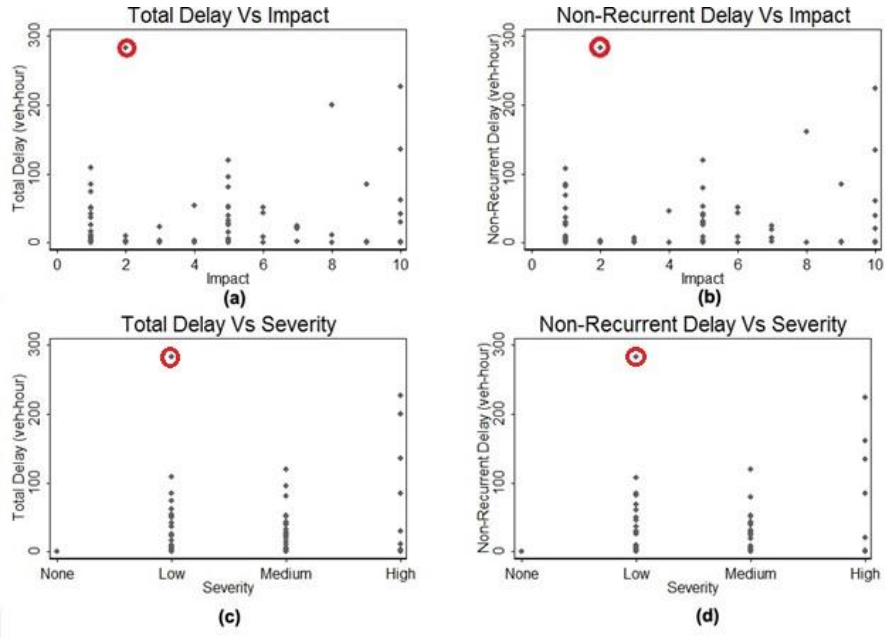

Figure 5-4 shows the relationship between the calculated delays and impact/severity based on operator's judgment. In general, the total delays increase as the level of impact/severity goes up, with exceptions highlighted in the graph (explained later). The averaged total delay for each level of impact is shown in Table 5-2.

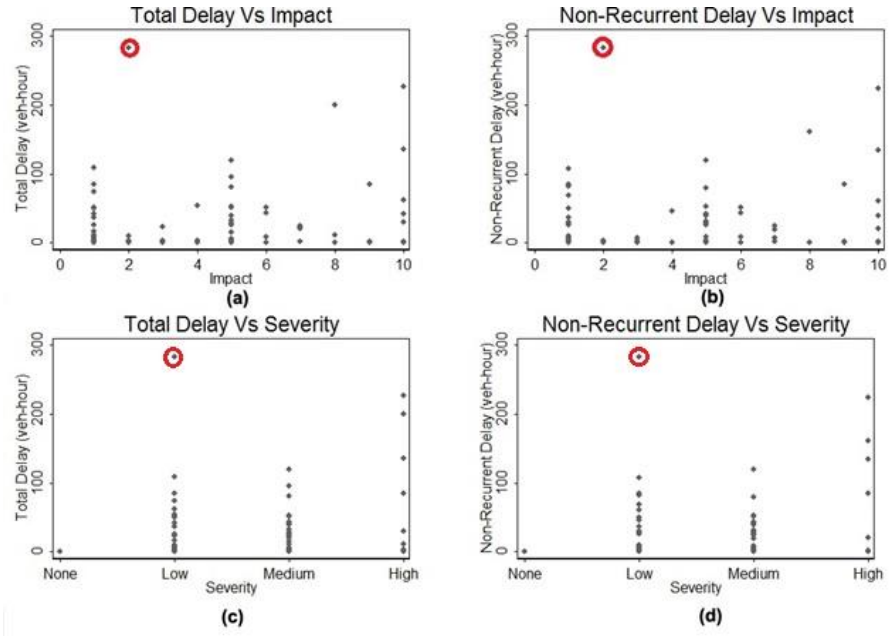

Figure 5-4 Relationship between Estimated Delay with Impact/Severity

Table 5-2 Comparison of Estimated Delay and Operator's Estimated Delay

Impact	1-3	4-6	7-10
Estimated Delay/Volume	<5 minute	5-15 minutes	>15 minutes
Averaged Total Delay/Volume	1.4 minutes	4.7 minutes	10.6 minutes

In Table 5-2, the average total delay is overall lower than the operator's judgment. Usually operators estimates the delay based on the severity of incidents. In our approach, we also consider the delay during the incident recovery period where the throughput starts to increase. As a result, the averaged total delay is consistently lower than operator's estimates.

Figure 5-5 presents the sum of total delay, IID, and number of incidents along the study corridor. Generally, incident hot spots have higher cumulative delay. Exceptions happened at MP 293, 296, and 307, where the numbers of incidents are significantly higher with relatively lower delay. This implies that at these locations suffer little overall congestion. Thus even with incidents, the traffic is not affected much. At MP 285, the number of incidents is less than the neighboring MPs, however, the delay is the highest throughout the entire segment, and incidents contribute most to the delay. Figure 5-6(a) shows the map of this location, which is at the on-ramp of I-15 from the Timpanogos Highway. The incidents are most likely attributable to the intensive weaving. The recurrent delays at MP 296 and 309 are higher comparing with other locations. As shown in Figure 5-6(b) and (c), MP 296 is at the Draper area, where the most severe recurrent congestion happens due to the densely populated residential neighborhood. MP 309 is the off-ramp from I-15 to W 600N. Recurrent delay happens due to the lane drop.

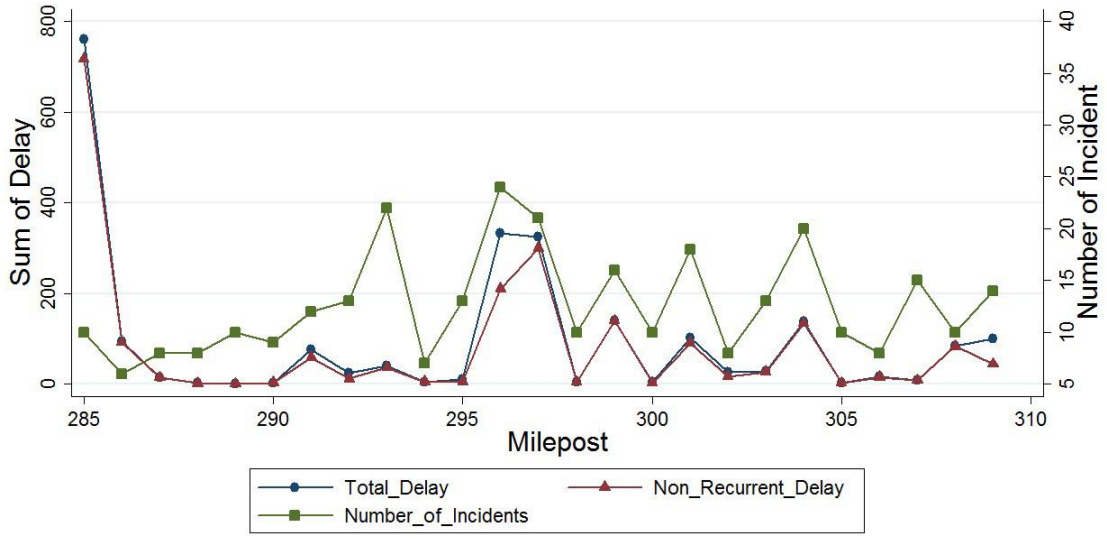

Figure 5-5 Summary of Total Delay, IID, and Number of Incidents along the Study Corridor

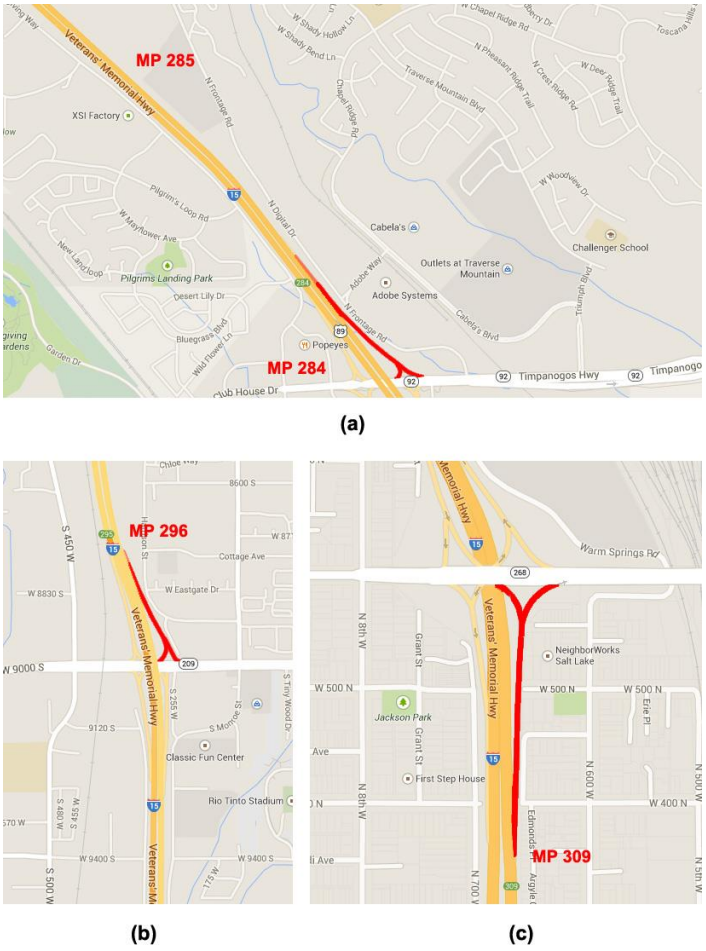

Figure 5-6 Locations of Incident Hotspots

5.5 Adverse Weather's Impact

To analyze the impact of adverse weather on the demand and capacity reduction, the weather data is first categorized by road and sky conditions. Figure 5-7 shows the histogram of weather record by road condition. Wet is the most frequently occurred road condition under adverse weather (60%) and slushy road condition accounts for approximately 15% of all the records. Figure 5-8 shows the histogram of sky condition of all the weather records. Snow is the most frequently occurring sky condition since the weather data was collected from November to December.

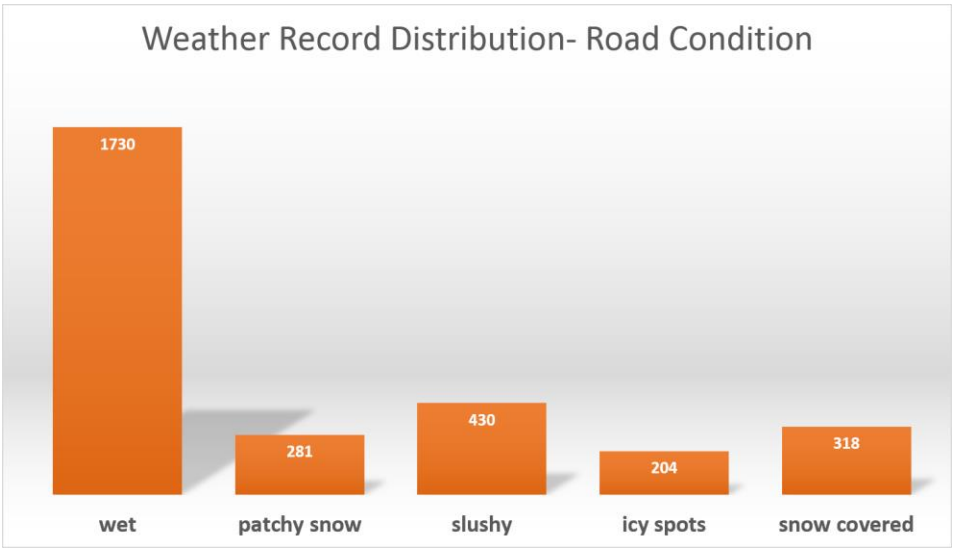

Figure 5-7 Histogram of Weather Observations by Road Condition

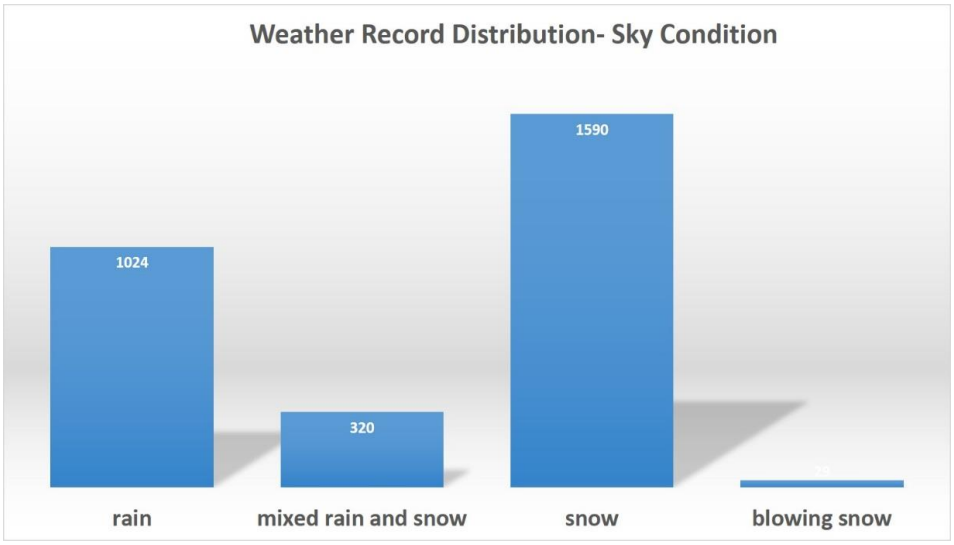

Figure 5-8 Histogram of Weather Observations by Sky Condition

For each weather record, we linked it with the PeMS traffic database by extracting speed, volume, and delay data in an effort to observe the pattern of the traffic. Figure 5-9 shows the plots of speed-flow data under different road conditions. It is noted that the speed-flow pattern would be able to demonstrate the severity of different weather and its impacts on the traffic. For example, when the roadway is wet, the speed flow pattern still follows the general parabolic curve where the distinctions between congested and uncongested regimes are observable. However, as the roadway condition gets worse, the normal pattern would become blurred and the

data are more randomly congregated. Particularly when the road is covered by snow, the scattered plot breaks down into two clusters.

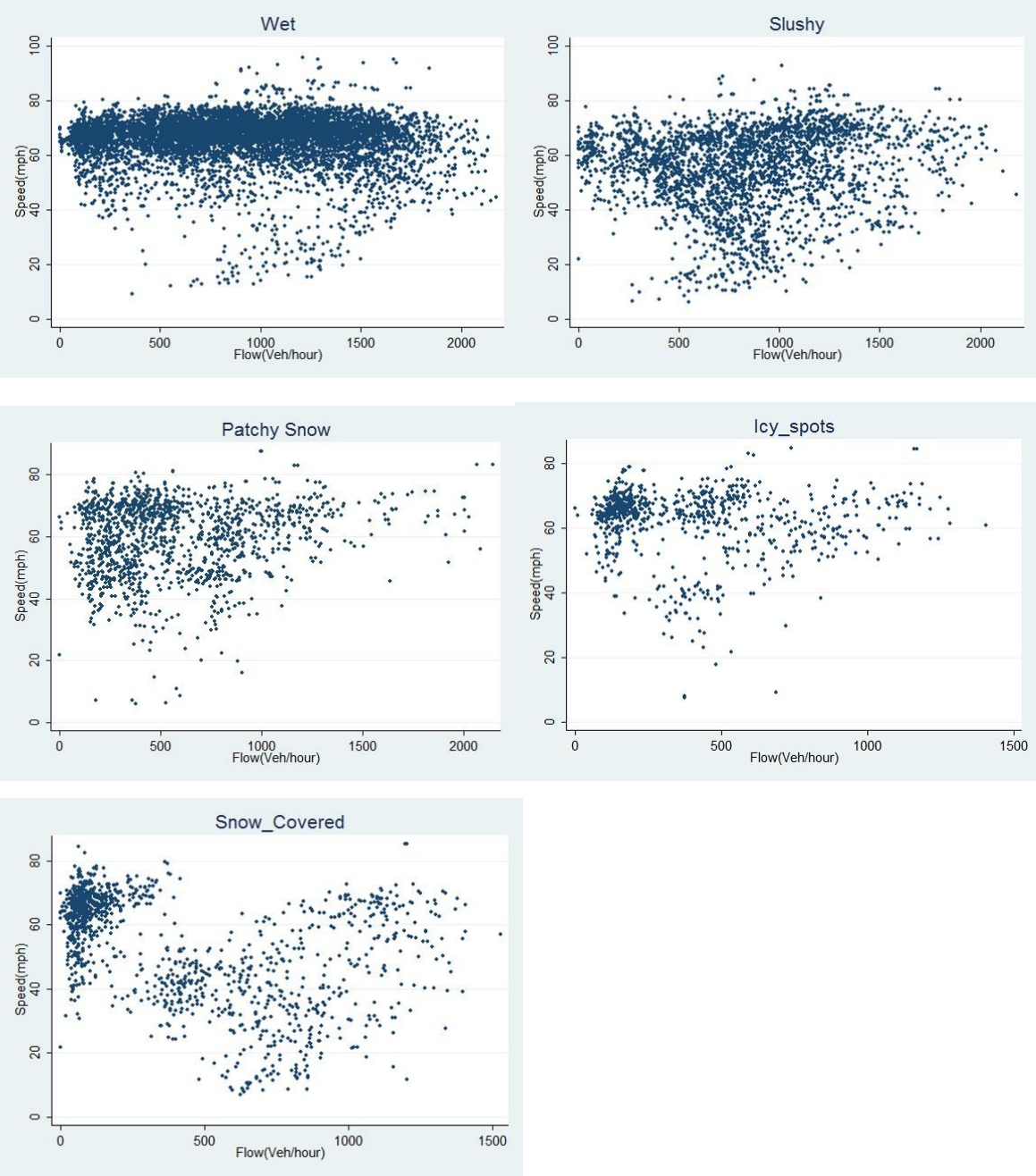

Figure 5-9 Traffic Flow Vs Speed Plots under Different Road Conditions

To quantitatively analyze the impact of adverse weather, the mechanism presented in Section 3.4 is applied to the dataset collected. Since $\Delta \mathrm{D}_{\mathrm{Wea}}(m,t,s,w)$ and $\Delta \mathrm{F}_{\mathrm{Wea}}(m,t,s,w)$ represent the delay and flow difference between the adverse weather and normal weather, they

can be used to classify the impact into different categories (expressed as ΔD and ΔF in the following section).

If $\Delta F > 0$ and $\Delta D > 0$, both volume and delay under normal conditions are higher than under adverse weather conditions, suggesting a demand reduction during adverse weather. If $\Delta F > 0$ and $\Delta D < 0$, volume under normal conditions is higher than under adverse weather, yet delay under normal conditions is lower than under adverse weather. It is caused by freeway capacity reduction during adverse weather. When $\Delta F < 0$ and $\Delta D > 0$, volume under normal conditions is lower than under adverse weather, and delay under normal conditions is higher than adverse weather. This situation would be quite counterintuitive and should be rarely observed in reality. When $\Delta F < 0$ and $\Delta D < 0$, both volume and delay under normal conditions are lower than under adverse weather, which means that the adverse weather does not have obvious impact on the freeway performance. In the following discussion, the four scenarios are referred as C1, C2, C3, and C4, separately. Table 5-3 shows the signs of ΔF and ΔD for each combination.

Table 5-3 Signs of ΔF and ΔD for Combinations of C1, C2, C3, C4

	C1	C2	C3	C4
ΔF	+	+	-	-
ΔD	+	-	+	-

Figure 5-10 shows the scattered ΔF and ΔD distribution under adverse weather during peak hours and non-peak hours. It's observed that during peak hours the distribution is more scattered than during non-peak hours. It demonstrates that the traffic during peak hours is more sensitive to disturbance than during non-peak hours, and any potential non-recurrent congestion source for is likely to induce higher fluctuations on both traffic volume and delay.

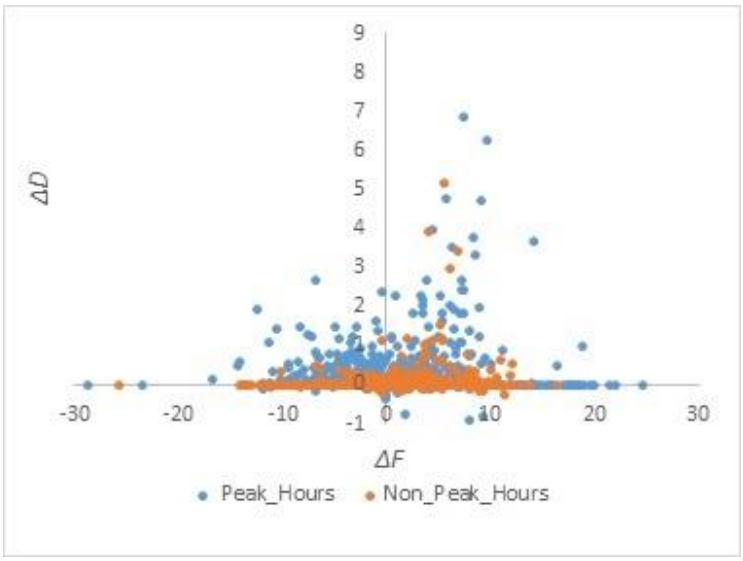

Figure 5-10 Scatter Plots of Δ*F* Vs. Δ*D* During Peak and Non-Peak Hours

Figure 5-11 shows the pie charts of the four ΔF and ΔD combination during peak hours and non-peak hours. For both scenarios, C1+C2 accounts for more than 90% of the cases, indicating volume under adverse weather is lower comparing with the normal days. C1 is the most frequently appeared situation, which shows that demand reduction is a major cause for the lower volume under adverse weather.

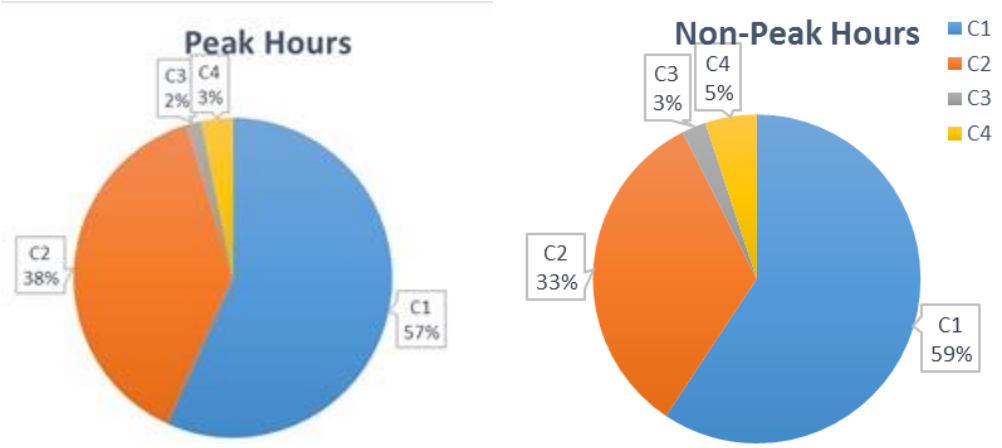

Figure 5-11 Comparison of Pie Charts during Peak and Non-Peak Hours

Figure 5-12 shows the pie charts for different road conditions during peak hours. As the road condition gets worse, the fractions of C1 increase, from 52% (wet road) to 71% (patchy snow). It is consistent with the fact that people trend to rearrange or cancel their trips when the weather gets worse.

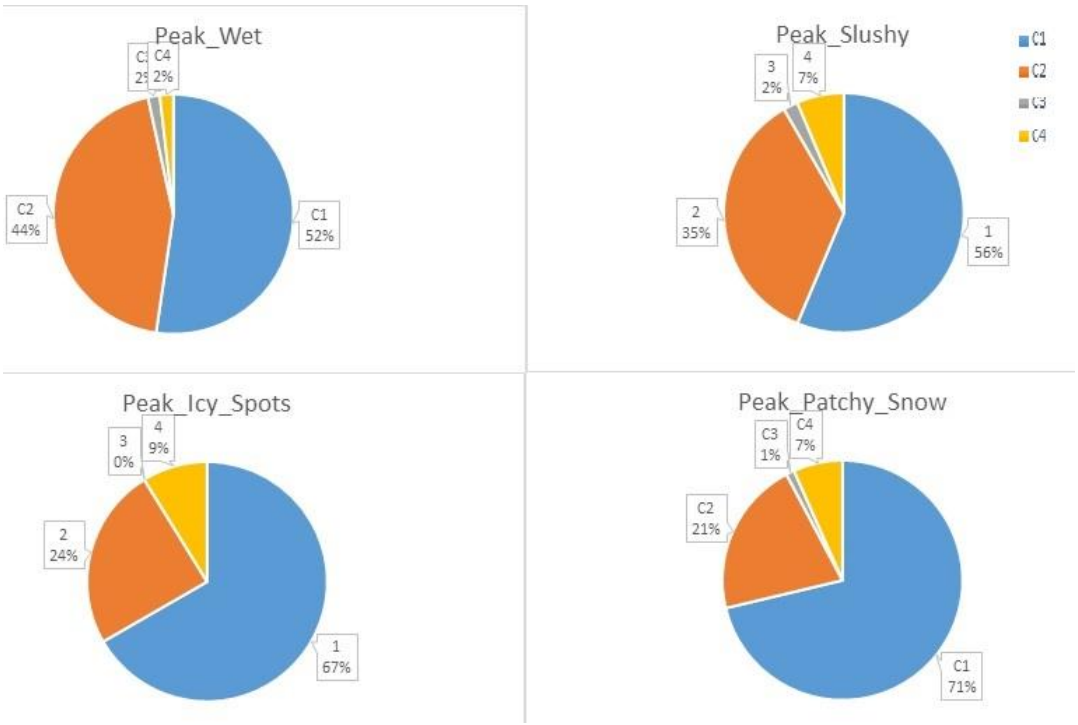

Figure 5-12 Combination Frequency during Peak Hours under Different Road Conditions.

5.6 Summary

In this Chapter, in-depth analysis of the three major tasks is performed using the data collected along the I-15 study corridor. The reliability analysis using congestion frequency allows the hot spots to be easily identified for different time periods. The congestion frequency index can be translated into the probability that a user will experience certain speed when he/she travels through a specific location. The unified measure is easy to interpret and implement for operational management. IID and secondary incident identification results are also presented in this chapter. During 2013, 7% of incidents that happened on the selected I-15 corridor were secondary incidents, which is lower than the 20% estimates given by FHWA. The occurrence of secondary incidents is highly related to adverse weather, where December has the highest number of the secondary incidents. The IID algorithm is applied to the 2013 incident dataset, and in general, high severity incidents would cause more delay with several exceptions due to the geometries of the roadway characteristics. The mechanism for quantifying the adverse weather impact is presented. The delay and volume estimators are applied to the 2013 winter adverse weather records. There are two major causes for the low volume during adverse weather. One is

the freeway capacity reduction caused by lowered speed, the other one is the demand reduction. The general parabolic curve of speed and volume does not hold when weather gets worse.

6.0 CONCLUSIONS

6.1 Summary

The focus of freeway performance measurements and monitoring is to describe the congestion and mobility of the roadway networks. Congestion levels are not the same every day. Especially under the impact of nonrecurring congestion sources, e.g. incident, work zone, and adverse weather, the associated congestion and its extent should be diagnosed with special attention. The purpose of this study is to provide data-driven solutions for evaluating the freeway performance under various scopes to assist with project prioritization and decision making. Freeway performance measures are oftentimes considered in three dimensions: temporal aspects, spatial details, and source of congestion. This study strives to address all three dimensions simultaneously. We start by developing a performance measure that is easy to understand and has practical implications. The measure, congestion frequency, ties to typical congestion levels and reliability to describe congestion/mobility performance of freeways, yet can be easily comprehended and related to by the general public based on their everyday experience. Once the unreliable locations are identified through the corridor performance analysis, attention is paid to have close scrutiny on the reasons for the unreliability. Incidents and adverse weather are considered as the main sources for nonrecurring congestion. Data-driven algorithms are developed to calculate IID and identify secondary incidents. The algorithms utilize spatiotemporal analysis to determine the impact range of each incident on the microscopic level, along with pattern matching and background subtraction methods to determine the recurrent congestion impact. To quantify the impact of adverse weather, a mechanism is developed by evaluating the volume and delay changes under both normal days and days with adverse weather. It is quantitatively proven that under snow-covered conditions, travel demand is decreased significantly.

6.2 Findings

The findings for the three major components carried through this project are summarized as follows.

6.2.1 Congestion Frequency Index

Congestion Frequency is presented as the measurement of performance reliability. We identified the hot spots on selected I-15 corridor in morning and evening peak hours during May to August 2013. Its pattern is consistent with speed percentiles, which is the current reliability measure used at TOC.

6.2.2 Secondary Incident Occurrence

Secondary incidents refer to the incidents that resulted from the congestion caused by previous incidents, including not only crashes, but also engine stalls, overheating, and running out of fuel scenarios. With the data-driven algorithm developed in this project, we identified 240 secondary incidents caused by 109 primary incidents on the selected I-15 corridor during 2013. The occurrence of secondary incidents follows a distinct seasonal pattern, where months with high precipitation (From Nov to March) have higher frequency of secondary incidents, while there were no secondary incidents identified for June, where the driest month was reported in Utah for the Years 1895-2013, according to National Climate Data Center. Reduced road friction and impaired visibility might be the main contributors for secondary incidents.

6.2.3 Hotspots on I-15 Corridor

The IID is not only determined by the severity of incident, but also dependent on the location and time of day. The locations with high incident frequency generally suffer from higher IID than the locations with low incident frequency. Exceptions happened at MP 284, MP 296, and MP 309 on Northbound I-15, where fewer incidents are observed with relatively high IID. These hotspots are usually located before off-ramps or after on-ramps connecting I-15 and arterials.

6.2.4 Mechanism of Adverse Weather Impacting Traffic

The results of adverse weather's impact analysis indicate that under the influence of adverse weather travel demand decreases, which is the case for more than 50% of the scenarios. We conclude that in 2013 the adverse weather forecasting system succeeded in alerting the public and preventing severe traffic breakdowns. As roadway condition gets worse, the traffic demand shows a more significant reduction pattern.

6.3 Recommendations

The data-driven performance-based approach presented in this study is effective in quantitatively evaluating the freeway mobility/reliability, incident and adverse weather impact. The objectives of this project align well with the goal set forth by MAP-21, which is to establish performance-based transportation programs to guide the transportation capital investment and development. The algorithm developed can be integrated into the operational analysis to identify hotspots along the freeway corridor, and assist with project prioritization and decision making. Future work involves evaluating the impact of other nonrecurring congestion sources identified by SHRP 2, including work zone, demand fluctuations, special events, traffic control devices, and inadequate base capacity. Also, since pattern matching algorithms are used in the analysis for determining the recurrent congestion from historical data, it is desirable to develop a web-based platform to allow operators/researchers to customize the duration of the historical data window to assist with interactively transportation analytics.

REFERENCES

Ahmed, Mohamed M, Mohamed Abdel-aty, Jaeyoung Lee, and Rongjie Yu. 2014. "Real-Time Assessment of Fog-Related Crashes Using Airport Weather Data : A Feasibility Analysis." *Accident Analysis and Prevention* 72: 309–317. doi:10.1016/j.aap.2014.07.004. http://dx.doi.org/10.1016/j.aap.2014.07.004.

Alvarez, Patricio, and Mohammed Hadi. 2012. "Time-Variant Travel Time Distributions and Reliability Metrics and Their Utility in Reliability Assessments." *Transportation Research Record: Journal of the Transportation Research Board* 2315: 81–88. doi:10.3141/2315-09. http://trb.metapress.com/openurl.asp?genre=article&id=doi:10.3141/2315-09.

Bergel-Hayat, Ruth, Mohammed Debbarh, Constantinos Antoniou, and George Yannis. 2013. "Explaining the Road Accident Risk: Weather Effects." *Accident Analysis and Prevention* 60: 456–465. doi:10.1016/j.aap.2013.03.006. http://dx.doi.org/10.1016/j.aap.2013.03.006.

Bertini, Robert L, and Galen E McGill. 2003. "Getting Traffic Moving Again." *Public Roads* 67 (2): 14–17.

Brijs, Tom, Dimitris Karlis, and Geert Wets. 2008. "Studying the Effect of Weather Conditions on Daily Crash Counts Using a Discrete Time-Series Model." *Accident Analysis and Prevention* 40: 1180–1190. doi:10.1016/j.aap.2008.01.001.

Cambridge Systematics. 2013. "Incorporating Reliability Performance Measures into the Transportation Planning and Programming Processes."

Chandana Wirasinghe, S. 1978. "Determination of Traffic Delays from Shock-Wave Analysis." *Transportation Research* 12 (5) (October): 343–348. doi:10.1016/0041-1647(78)90010-2. http://www.sciencedirect.com/science/article/pii/0041164778900102.

Chung, Younshik. 2012. "Assessment of Non-Recurrent Congestion Caused by Precipitation Using Archived Weather and Traffic Flow Data." *Transport Policy* 19 (1): 167–173. doi:10.1016/j.tranpol.2011.10.001. http://dx.doi.org/10.1016/j.tranpol.2011.10.001.

Chung, Younshik. 2013. "Identifying Primary and Secondary Crashes from Spatiotemporal Crash Impact Analysis." *Transportation Research Record: Journal of the Transportation Research Board* 2386 (-1) (December 1): 62–71. doi:10.3141/2386-08. http://trb.metapress.com/openurl.asp?genre=article&id=doi:10.3141/2386-08.

Datla, Sandeep, and Satish Sharma. 2008. "Impact of Cold and Snow on Temporal and Spatial Variations of Highway Traffic Volumes." *Journal of Transport Geography* 16: 358–372. doi:10.1016/j.jtrangeo.2007.12.003.

Edwards, Matthew B., and Michael D. Fontaine. 2012. "Investigation of Travel Time Reliability in Work Zones with Private-Sector Data." *Transportation Research Record: Journal of the Transportation Research Board* 2272: 9–18. doi:10.3141/2272-02.

El-basyouny, Karim, Sudip Barua, and Tazul Islam. 2014. “Investigation of Time and Weather Effects on Crash Types Using Full Bayesian Multivariate Poisson Lognormal Models.” *Accident Analysis and Prevention* 73: 91–99. doi:10.1016/j.aap.2014.08.014. http://dx.doi.org/10.1016/j.aap.2014.08.014.

Emam, Emam, and Haitham AI-Deek. 2006. “Using Real-Life Dual-Loop Detector Data to Develop New Methodology for Estimating Freeway Travel Time Reliability.” *Transportation Research Record* 1959 (1959): 140–150. doi:10.3141/1959-16.

Guo, Feng, Qing Li, and Hesham Rakha. 2012. “Multistate Travel Time Reliability Models with Skewed Component Distributions.” *Transportation Research Record: Journal of the Transportation Research Board* 2315 (-1) (December 1): 47–53. doi:10.3141/2315-05. http://trb.metapress.com/openurl.asp?genre=article&id=doi:10.3141/2315-05.

Hallenbeck, Mark E, John M Ishimaru, Jennifer Nee, and Toby D Rickman. 2003. “Measurement of Recurring Versus Non-Recurring Congestion.”

Keay, Kevin, and Ian Simmonds. 2005. “The Association of Rainfall and Other Weather Variables with Road Traffic Volume in Melbourne, Australia.” *Accident Analysis and Prevention* 37: 109–124. doi:10.1016/j.aap.2004.07.005.

Khattak, Asad, Xin Wang, and Hongbing Zhang. 2009. “Are Incident Durations and Secondary Incidents Interdependent?” *Transportation Research Record: Journal of the Transportation Research Board* 2099 (-1) (January 1): 39–49. doi:10.3141/2099-05. http://trb.metapress.com/openurl.asp?genre=article&id=doi:10.3141/2099-05.

Kwon, Jaimyoung, Michael Mauch, and Pravin Varaiya. 2006. “Components of Congestion: Delay from Incidents, Special Events, Lane Closures, Weather, Potential Ramp Metering Gain, and Excess Demand.” *Transportation Research Record* 1959 (1) (January 1): 84–91. doi:10.3141/1959-10. http://trb.metapress.com/openurl.asp?genre=article&id=doi:10.3141/1959-10.

Li, Jibing, Chang-jen Lan, and Xiaojun Gu. 2006. “Estimation of Incident Delay and Its Uncertainty on Freeway Networks.” *Transportation Research Record: Journal of the Transportation Research Board*: 37–45.

Liu, Henry X., Xiaozheng He, and Will Recker. 2007. “Estimation of the Time-Dependency of Values of Travel Time and Its Reliability from Loop Detector Data.” *Transportation Research Part B: Methodological* 41 (4) (May): 448–461. doi:10.1016/j.trb.2006.07.002. http://linkinghub.elsevier.com/retrieve/pii/S0191261506000890.

Lyman, Kate, and Robert L. Bertini. 2008. “Using Travel Time Reliability Measures to Improve Regional Transportation Planning and Operations.” *Transportation Research Record: Journal of the Transportation Research Board* 2046 (-1) (December 1): 1–10. doi:10.3141/2046-01. http://trb.metapress.com/openurl.asp?genre=article&id=doi:10.3141/2046-01.

Mahmassani, Hani S., Tian Hou, and Jing Dong. 2012. “Characterizing Travel Time Variability in Vehicular Traffic Networks.” *Transportation Research Record: Journal of the Transportation Research Board* 2315 (-1) (December 1): 141–152. doi:10.3141/2315-15. http://trb.metapress.com/openurl.asp?genre=article&id=doi:10.3141/2315-15.

Maze, Thomas, Manish Agarwai, and Garrett Burchett. 2006. “Whether Weather Matters to Traffic Demand, Traffic Safety, and Traffic Operations and Flow.” *Transportation Research Record* 1948: 170–176. doi:10.3141/1948-19.

Mehran, Babak, and Hideki Nakamura. 2009. “Implementing Travel Time Reliability for Evaluation of Congestion Relief Schemes on Expressways.” *Transportation Research Record: Journal of the Transportation Research Board* 2124 (-1) (December 1): 137–147. doi:10.3141/2124-13. http://trb.metapress.com/openurl.asp?genre=article&id=doi:10.3141/2124-13.

Mongeot, Hélène, and Jean-Baptiste Lesort. 2000. “Analytical Expressions of Incident-Induced Flow Dynamics Perturbations: Using Macroscopic Theory and Extension of Lighthill-Whitham Theory.” *Transportation Research Record: Journal of the Transportation Research Board* 1710 (1): 58–68.

Pu, Wenjing. 2011. “Analytic Relationships Between Travel Time Reliability Measures.” *Transportation Research Record: Journal of the Transportation Research Board* 2254 (1) (December 1): 122–130. doi:10.3141/2254-13. http://trb.metapress.com/openurl.asp?genre=article&id=doi:10.3141/2254-13.

Saberi, Meead, and Robert L Bertini. 2010. “Beyond Corridor Reliability Measures : Analysis of Freeway Travel Time Reliability at the Segment Level for Hotspot Identification” 514 (July 2009): 1–13.

Skabardonis, Alexander, Pravin Varaiya, and Karl F Petty. 2003. “Measuring Recurrent and Nonrecurrent Traffic Congestion.” *Transportation Research Record: Journal of the Transportation Research Board* 1856 (1): 118–124. doi:10.3141/1856-12.

Thakuriah, Piyushimita (Vonu), and Nebiyou Tilahun. 2012. “Incorporating Weather Information into Real-Time Speed Estimates: Comparison of Alternative Models.” *Journal of Transportation Engineering* (April): 121001063128003. doi:10.1061/(ASCE)TE.1943-5436.0000506.

Tu, Huizhao, Adam J. Pel, Hao Li, and Lijun Sun. 2012. “Travel Time Reliability During Evacuation.” *Transportation Research Record: Journal of the Transportation Research Board* 2312 (-1) (December 1): 128–133. doi:10.3141/2312-13. http://trb.metapress.com/openurl.asp?genre=article&id=doi:10.3141/2312-13.

Van Aerde, Michel, and Hesham Rakha. 1995. “Multivariate Calibration of Single Regime Speed-Flow-Density Relationships.” In *Proceedings of the 6th 1995 Vehicle Navigation and Information Systems Conference*, 334–341.

Van Lint, J., and H. Van Zuylen. 2005. “Monitoring and Predicting Freeway Travel Time Reliability: Using Width and Skew of Day-to-Day Travel Time Distribution.” *Transportation Research Record* 1917 (1) (January 1): 54–62. doi:10.3141/1917-07. http://trb.metapress.com/openurl.asp?genre=article&id=doi:10.3141/1917-07.

Wang, Yinhai, Patikhom Cheevarunothai, and Mark Hallenbeck. 2008. “Quantifying Incident-Induced Travel Delays on Freeways Using Traffic Sensor Data.”

Yang, Hong, Bekir Bartin, and Kaan Ozbay. 2013. “Use of Sensor Data to Identify Secondary Crashes on Freeways.” *Transportation Research Record: Journal of the Transportation Research Board* 2396 (-1) (December 1): 82–92. doi:10.3141/2396-10. http://trb.metapress.com/openurl.asp?genre=article&id=doi:10.3141/2396-10.

Yang, and Will Recker. 2005. “Simulation Studies of Information Propagation in a Self-Organizing Distributed Traffic Information System.” *Transportation Research Part C: Emerging Technologies* 13 (5-6) (October): 370–390. doi:10.1016/j.trc.2005.11.001. http://linkinghub.elsevier.com/retrieve/pii/S0968090X05000550.

Yu, Rongjie, Mohamed Abdel-Aty, and Mohamed Ahmed. 2013. “Bayesian Random Effect Models Incorporating Real-Time Weather and Traffic Data to Investigate Mountainous Freeway Hazardous Factors.” *Accident Analysis and Prevention* 50: 371–376. doi:10.1016/j.aap.2012.05.011. http://dx.doi.org/10.1016/j.aap.2012.05.011.

Yu, Runze, Yunteng Lao, Xiaolei Ma, and Yinhai Wang. 2014. “Short-Term Traffic Flow Forecasting for Freeway Incident-Induced Delay Estimation.” *Journal of Intelligent Transportation Systems* 18 (3) (May 23): 254–263. doi:10.1080/15472450.2013.824757. http://dx.doi.org/10.1080/15472450.2013.824757.